Theoretical Notes
Note 237

TN
237

SLA-74-0191
Unlimited Release
Printed June 1974

EXPANSION METHOD FOR CALCULATING DISPERSION OF ELECTROMAGNETIC PULSES PROPAGATING IN THE IONOSPHERE

C. N. Vittitoe
Theoretical Division, 5223
Sandia Laboratories
Albuquerque, New Mexico 87115

ABSTRACT

An expansion method for calculating the effect of dispersion upon electromagnetic pulses propagating through the ionosphere is applied to a double-exponential pulse. It may, however, be applied to any incident pulse that can be represented by a Fourier series. The phase angle introduced by the transmission medium is expanded in a Taylor series, which is truncated after the second-order dispersion term. Unlike many treatments of ionospheric propagation, the large-dispersion approximation is not made. In some cases the dispersed-pulse durations are greater than the times between arrivals of the various frequency components. The components then interfere to form quite complicated waveforms. It is found that the high-frequency, low-dispersion components often add constructively to produce the maximum amplitude in the transmitted signal. Equations are presented for frequency-domain analysis of the signal, but results are given in the time domain. Appendixes outline a rapid method for calculation of the Fresnel integral and its auxiliary functions; present results for propagation of the double-exponential pulse through a series of atmospheric ionizations; and illustrate the contributions of individual frequency components, as well as the effect of correction factors to account for the possibility of low dispersion of some frequency components.

ACKNOWLEDGMENT

The author gratefully acknowledges the assistance of R. Lighthill and F. Biggs in providing quadratic spline fits for ionospheric parameters, and helpful discussions with R. D. Jones and W. A. Radasky concerning methods of calculating Fresnel integrals and the general propagation problem.

TABLE OF CONTENTS

LIST OF ILLUSTRATIONS

EXPANSION METHOD FOR CALCULATING DISPERSION OF ELECTROMAGNETIC PULSES PROPAGATING IN THE INOSPHERE

Introduction

In the past several years, interest has been growing in the vulnerability of satellites to nuclear weapon effects. One of these threats is the electromagnetic pulse (EMP) radiated from a nuclear explosion. The purpose of this report is to illustrate a method for calculating the effect of ionospheric dispersion upon such an electromagnetic pulse. A series of results of this method is also presented.

The problem of pulse propagation in an ionized medium has been considered by many authors. In fact, a treatment of propagation in and reflection from the ionosphere is included in a classic work by Ginzburg.[1]

Jones and Ring have recently found that dispersion effects dominate those of energy absorption for EMP-type waveforms propagating through the ionosphere.[2] Messier, regarding the problem with the assumption of high dispersion, indicates that (1) the effects of the ionosphere are more easily represented in the frequency domain and (2) in most calculations of coupling the energy into a satellite, the frequency domain is the most convenient for analysis. Messier also presents results in the time domain.[3] The present work differs from that presented in References 2 and 3 in that the time-domain-propagated signals are calculated with a series representation of the incident pulse, without the assumption of large dispersion. The method illustrated here has also been applied to other waveforms for use in a satellite vulnerability computer code developed by Sandia Laboratories.[4]

When one is calculating nuclear-weapon environments, a conservative approach is usually taken to justify the conclusion that a certain system will survive. Hence, the ionospheric plasma absorption of energy is omitted, and absorption effects are dominated by those of dispersion. By omitting the real part of the ionospheric conductivity, one avoids the nonlinear effects of the electric-field-dependent air conductivity. Linear theory can then be used and the wave can be expressed as a Fourier integral.

Incident Pulse

Let us consider the incident pulse

$$E_i(t) = \left\{ c_o + \sum_{k=1}^{K} c_k \cos(\omega_k t + \varphi_k) \right\} \left[U(t) - U(t - T) \right], \tag{1}$$

where $\omega_k = 2\pi k/T_o$, $N_1 T_o = T$, and U is the Heaviside unit step function. Here N_1 is an integer and T is the pulse duration. The coefficients and phase are readily evaluated by $c_o = |a_o'|$, $c_k = 2|a_k'|$ and $\varphi_k = \tan^{-1}[\text{Im } a_k'/\text{Re } a_k']$, where

$$a_k' \equiv \frac{1}{T}\int_o^T E_i(\tau)e^{-i\omega_k\tau}\,d\tau \ . \tag{2}$$

An equivalent representation of the pulse is

$$E_i(t) = \sum_{k=0}^{K} A_k(t)e^{i\omega_k t} \ , \tag{3}$$

where

$$A_k(t) = c_k e^{i\varphi_k}\left[U(t) - U(t - T)\right] . \tag{4}$$

As indicated by Ginzburg, this form is convenient for some of the mathematical manipulation.[1] In terms of the Fourier transform,

$$E_i(t) = \int_{-\infty}^{\infty} g(\omega)e^{i\omega t}\,d\omega \tag{5}$$

with

$$g(\omega) = \frac{1}{2\pi}\int_{-\infty}^{\infty} E_i(t)e^{-i\omega t}\,dt \ . \tag{6}$$

From Eqs. (3)-(6)

$$g(\omega) = \frac{1}{2\pi i}\sum_{k=0}^{K} c_k e^{i\varphi_k}\,\frac{\exp\left[i(\omega_k - \omega)T\right] - 1}{(\omega_k - \omega)} \ . \tag{7}$$

Thus, $g(\omega)$ has the appearance of a series of quasi-monochromatic signals with angular frequency ω_k. The spectral width of each frequency component is $\Delta\omega \approx \omega_k$. At $\omega \approx \omega_k$,

$$g(\omega_k) = (2\pi)^{-1} T c_k e^{i\varphi_k} \ .$$

The specific pulse chosen here for analysis is the standard double-exponential pulse

$$E(t) = \left(e^{-at} - e^{-bt}\right)U(t) \ . \tag{8}$$

For this pulse, as found by Jones and Ring,[2]

$$c_o = \frac{1}{aT}\left(1-e^{-aT}\right) + \frac{1}{bT}\left(1-e^{-bT}\right),$$

$$c_k = \frac{2}{T}\left\{\left[\frac{-a}{a^2+\omega_k^2}\left(e^{-aT}-1\right) + \frac{b}{b^2+\omega_k^2}\left(e^{-bT}-1\right)\right]^2 + \left[\frac{\omega_k}{a^2+\omega_k^2}\left(e^{-aT}-1\right) - \frac{\omega_k}{b^2+\omega_k^2}\left(e^{-bT}-1\right)\right]^2\right\}^{1/2}, \tag{9}$$

$$\varphi_k = \tan^{-1}\frac{\omega_k\left(b^2+\omega_k^2\right)\left(e^{-aT}-1\right) - \omega_k\left(a^2+\omega_k^2\right)\left(e^{-bT}-1\right)}{-a\left(b^2+\omega_k^2\right)\left(e^{-aT}-1\right) + b\left(a^2+\omega_k^2\right)\left(e^{-bT}-1\right)}.$$

Obviously, however, Eq. (2) makes the method readily adaptable to an arbitrary incident pulse, $E_i(\tau)$.

Possible Forms of the Transmitted Pulse

After transmission through the ionosphere, the pulse may be represented by

$$E(t) = \int_{-\infty}^{\infty} g(\omega)\, R(\omega)\, e^{i\omega t}\, d\omega, \tag{10}$$

where $R(\omega)$ is the response function of the ionosphere, $R(\omega) = |R(\omega)|\, e^{-i\varphi(\omega)}$. Disregard of the ionospheric attenuation gives $|R(\omega)| = 1$. If, as suggested by Eq. (7), it is assumed that $g(\omega)$ is a superposition of quasi-monochromatic sources, the phase factor may be expanded in a Taylor series about ω_k as follows:

$$\varphi(\omega) = \varphi(\omega_k) + (\omega-\omega_k)\,\varphi'(\omega_k) + \frac{1}{2}(\omega-\omega_k)^2\,\varphi''(\omega_k) + \frac{1}{6}(\omega-\omega_k)^3\,\varphi'''(\omega_k) + \ldots. \tag{11}$$

Combining Eqs. (3), (5), (6), and (10) yields

$$E(t) = \frac{1}{2\pi}\sum_{k=0}^{K}\int_{-\infty}^{\infty}\int_{-\infty}^{\infty} A_k(\eta)\exp\{i[(\omega_k-\omega)\eta + \omega t - \varphi]\}\, d\eta d\omega. \tag{12}$$

Substitution for φ from Eq. (11), with $\Omega = \omega - \omega_k$, gives

$$E(t) = \sum_{k=0}^{K}\frac{\exp\{i[\omega_k t - \varphi(\omega_k)]\}}{2\pi}\int_{-\infty}^{\infty}\int_{-\infty}^{\infty} A_k(\eta)\, e^{i\Omega'}\, d\eta\, d\Omega,$$

where

$$\Omega' = \Omega(t - \eta - \varphi') - \frac{\Omega^2 \varphi''}{2} - \frac{\Omega^3 \varphi'''}{6} + \ldots \ .$$

With φ given by Eq. (11) and the substitutions $\pi \xi^2 = \left(\Omega + \frac{\eta - t + \varphi'}{\varphi''}\right)^2 \varphi''$ and $T_k = [\pi \varphi'' (\omega_k)]^{1/2}$,* the transmitted pulse becomes

$$E(t) = \frac{1}{2} \sum_{k=0}^{K} \frac{\exp\{i[\omega_k t - \varphi(\omega_k)]\}}{T_k} \int_{-\infty}^{\infty} A_k(\eta) \exp\left[i \frac{(\eta - t + \varphi')^2}{2\varphi''}\right]$$

$$\times \int_{-\infty}^{\infty} \exp\left[-\frac{i\pi\xi^2}{2} - \frac{i\Omega^3 \varphi'''}{6} + \ldots\right] d\xi d\eta \ , \tag{13}$$

where

$$\Omega = T_k \xi - \eta + t - \varphi'(\omega_k) \ .$$

In order to evaluate Eq. (13), it is most convenient to use as few terms as possible in both the summation over k and in the expansion of the exponent in the integrand. Setting φ''' and higher order terms equal to zero, with $\int_{-\infty}^{\infty} \exp(-i\pi\xi^2/2)\, d\xi = 1 - i$ and $\pi u^2/2 = (\eta - t + \varphi')^2/2\varphi''$, gives the approximation designated by the subscript a1:

$$E_{a1}(t) = \frac{1 - i}{2} \sum_{k=0}^{K} \exp\{i[\omega_k t - \varphi(\omega_k)]\} \int_{-\infty}^{\infty} A_k(t - \varphi' + T_k u)\, e^{i\pi u^2/2}\, du \ . \tag{14}$$

If φ'' can also be disregarded,

$$E_{a2}(t) = \sum_{k=0}^{K} A_k(t - \varphi') \exp\{i[\omega_k t - \varphi(\omega_k)]\} \ . \tag{15}$$

From this form the group delay time is defined by $\Delta t_{gr} = \varphi'$, and the phase angle delay is $\varphi(\omega_k)$.

As discussed by Ginzburg[1] the total phase in Eq. (11) must change sign for $\omega < 0$. The $g(\omega)$, however, is appreciable only in the vicinity of each positive ω_k. Hence, Eq. (12) may be replaced by

$$E(t) = \frac{1}{2\pi} \sum_{k=0}^{K} \int_{0}^{\infty} \int_{-\infty}^{\infty} A_k(\eta) \exp[i(\omega_k - \omega)\eta + \omega t - \varphi] d\eta d\omega \ ,$$

*When $\varphi'' < 0$, $T_k \equiv [\pi |\varphi''(\omega_k)|]^{1/2}$.

and with Ω and ξ as before,

$$E(t) = 1/2 \sum_{k=0}^{K} \frac{\exp\{i[\omega_k t - \varphi(\omega_k)]\}}{T_k} \int_{-\infty}^{\infty} A_k(\eta) \exp\left[i \frac{(\eta - t + \varphi')^2}{2\varphi''}\right]$$

$$\times \int_{\xi_1}^{\infty} \exp\left[-\frac{i\pi\xi^2}{2} - \frac{i\Omega^3\varphi'''}{6} + \ldots\right] d\xi\, d\eta,$$

where

$$\xi_1 = \frac{1}{T_k}\left(-\omega_k|\varphi''| + \eta - t + \varphi'\right).$$

Again if φ''' can be disregarded, the resulting approximation is

$$E_{a3}(t) = \sum_{k=0}^{K} \frac{\exp\{i[\omega_k t - \varphi(\omega_k)]\}}{2\,T_k} \int_{-\infty}^{\infty} A_k(\eta) \exp\left[i \frac{(\eta - t + \varphi')^2}{2\varphi''}\right] \times [F^*(\infty) - F^*(\xi_1)]d\eta \tag{16}$$

where F^* is the complex conjugate of the Fresnel integral,

$$F(z) = \int_0^z e^{i\pi u^2/2}\, du \tag{17}$$

and $F(\infty) = (1 + i)/2$. The real and imaginary parts are identified by $F(z) = C(z) + i\,S(z)$. With A_k given by Eq. (4) and u as before, the approximation becomes

$$E_{a3}(t) = \sum_{k=0}^{K} \frac{c_k e^{i\varphi_k}}{2} \exp\{i[\omega_k t - \varphi(\omega_k)]\} \times \int_{-\theta_k/T_k}^{(T-\theta_k)/T_k} e^{i\pi u^2/2}\left[\frac{1 - i}{2} - F^*(\xi_1)\right] du\,, \tag{18}$$

where $\xi_1 = u - \omega_k T_k/\pi$ and $\theta_k = t - \varphi'(\omega_k)$. The θ_k measures time from the arrival of the frequency component ω_k. For $\theta_k < 0$, the k^{th} component has not yet had sufficient time to contribute to the signal. If $-\xi_1$ remains large and positive throughout the range of integration $-F^*(\xi_1) \approx (1 - i)/2$ and the approximation reduces to the simpler form,

$$E_{a4}(t) = \frac{1 - i}{2} \sum_{k=0}^{K} c_k \exp\{i[\omega_k t + \varphi_k - \varphi(\omega_k)]\}\left[F\left(\frac{T - \theta_k}{T_k}\right) + F\left(\frac{\theta_k}{T_k}\right)\right]. \tag{19}$$

This is similar to the results obtained by Jones and Ring[2] and by Ginzburg.[1] The transmitted pulse is given by the sum of its quasi-monochromatic-frequency components. With large dispersion the frequency components do not interfere with each other. At large θ_k the sum of the Fresnel integrals effectively reduces the signal to negligible values. The frequency components are shifted in phase by the original φ_k obtained from the incident pulse plus the $\omega_k t$ and the phase change caused by the ionosphere, $\varphi(\omega_k)$. It remains to be seen which of the approximations are valid for an EMP propagating through a model ionosphere.

Model Ionosphere

In order to obtain a reasonable underestimate of the effect upon pulses propagating through the ionosphere, the electron density must represent a lower limit. Density data given by Price have been represented by the function[5]

$$N = 3.4 \times 10^8 \exp[(z - 90.)/5.] \qquad z < 90 \text{ km},$$

$$N = 10^6 \times \exp(y_1) \qquad 90 \le z < 1200 \text{ km},$$

$$N = 4. \times 10^9 \exp[(1200. - z)/400.] \qquad z \ge 1200 \text{ km},$$

where the altitude z is in km, N is in electrons/m^3, and y_1 is given by the quadratic spline fit obtained from the UNFOLD program,[6]

$$y_1 = \alpha_1 + \alpha_2 z + \alpha_3 z^2 + \sum_{i=4}^{12} \alpha_i (z - \beta_i)^2 U(z - \beta_i) . \tag{20}$$

Here U is again the Heaviside unit step function.

The total electron content (TEC) is defined by

$$\text{TEC} \equiv \int_0^{\ell} N \, ds ,$$

where ds is the element of path length. If the integral is evaluated along a vertically upward path originating at the earth's surface, with N as given above, the TEC can be represented by

$$\text{TEC} = 1.7\text{E}12 \times \{\exp[(z - 90.)/5.] - \exp[-18.]\} \qquad z < 90 \text{ km},$$

$$\text{TEC} = \exp(y_2) \qquad 90 \le z < 1200 \text{ km},$$

$$\text{TEC} = 2.66321\text{E}16 + 1.6\text{E}15 \times \{1. - \exp[(1200. - z)/400.]\} \qquad z \ge 1200 \text{ km},$$

where z is in km, TEC is in electrons/m^2, and y_2 is given as in Eq. (20) with α_i replaced by γ_i and β_i replaced by δ_i. The coefficients are given in Table I. The functions are illustrated in Figure 1. The simpler character of the TEC allows it to be represented by 9 coefficients rather than the 12 in Eq. (20).

TABLE I

Spline Fit Parameters for Evaluating N and TEC

i	α_i	β_i (km)	γ_i	δ_i (km)
1	1.21272536E+3	-	-9.48153500E+0	-
2	-2.70199204E+1	-	6.60216709E-1	-
3	1.51221780E-1	-	-2.67240111E-3	-
4	-1.79349489E-1	90.5	2.70437824E-3	120.
5	4.83587886E-2	98.	8.94020605E-5	180.
6	-2.03333842E-2	100.	-3.54413041E-4	260.
7	8.56362240E-4	150.	2.22781492E-4	340.
8	-6.95992291E-4	175.	7.99615955E-6	500.
9	-6.16064716E-4	250.	2.34756800E-6	800.
10	5.68932804E-4	300.	-	-
11	-7.82182710E-6	500.	-	-
12	-1.84230226E-5	1150.	-	-

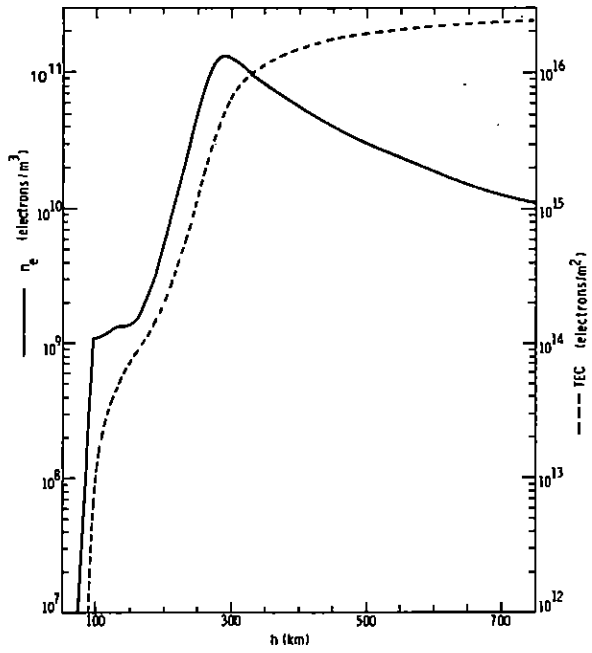

Figure 1. Electron Density and TEC for a Vertically Upward Path as a Function of Altitude Above the Earth's Surface

As indicated in the introduction, attenuation of the wave is ignored. Hence, the index of refraction for the ionosphere is a real quantity given by[7]

$$n = \sqrt{1 - \omega_p^2/\omega^2} \quad , \tag{21}$$

where the plasma frequency is

$$\omega_p^2 = \frac{Ne^2}{\epsilon_o m_e} = 3.18253 \times 10^3 \ m^3/s^2 \times N .$$

This expression also disregards geomagnetic complications, which should be taken into account for $\omega \lesssim \omega_B$. Since $\omega_B = eB_o/m_e \lesssim 5 \times 10^6$ rad/s, Eq. (21) is restricted to $\omega > 5 \times 10^6$ rad/s. At the peak of the modeled ionospheric electron density, $N = 1.4 \times 10^{11}$ electrons/m^3; the resulting plasma frequency is $\omega_p = 2.1 \times 10^7$ rad/s. Smaller frequencies result in an imaginary index of refraction; hence, smaller frequencies cannot propagate through the ionosphere. The index of refraction is illustrated in Figure 2. As indicated by Messier[3] and by Ginzburg,[1] other geometrical factors occur in calculating the minimum frequency propagating obliquely through the ionosphere. In that case the cut-off, or critical frequency, is $\omega_c = \omega_p/\cos\theta_o$ where θ_o is the angle between the ray path and the vertical at entrance to the ionosphere (the angle of incidence). Also, in the case of oblique rays, differing of the paths for the various frequency components will result in slightly larger TEC values and larger delay (both because of the TEC and the larger distance traveled) for the lower frequency components. For reflected rays the lower frequency components travel less distance. Consistent with the conservative approach, however, these variations of TEC and z are omitted from further consideration.

Figure 1 suggests that calculations of propagation in the model ionosphere should include TEC values in the range $10^{14} \le$ TEC $\le 2.5 \times 10^{16}$ electrons/m^2. However, the definition of TEC just below Eq. (20) indicates that for an oblique path through the ionosphere the TEC is increased above the vertical path value by a geometrical factor. With h_1 and h_2 the altitudes of the lower limit taken for the ionosphere and for the end of the propagation path, respectively, with ℓ_1 and ℓ_2 the distances from the origin as indicated in Figure 3, and with θ as defined in the same figure, the increase in TEC caused by the geometrical factor is $(\ell_2 - \ell_1)/(h_2 - h_1)$, as indicated in Figure 4 for $h_1 = 90$ km and a series of h_2 values. In Figure 4 R_e is the 6371-km radius of the earth. The formulas in Figure 4 assume straight-line propagation, inasmuch as frequency dependence would have to be included in order to take path curvature into account. The figure indicates that the TEC values considered should extend to $\sim 10^{17}$ electrons/m^2. In Appendix B the TEC values are extended still higher in view of the minimum ionosphere chosen as a model.

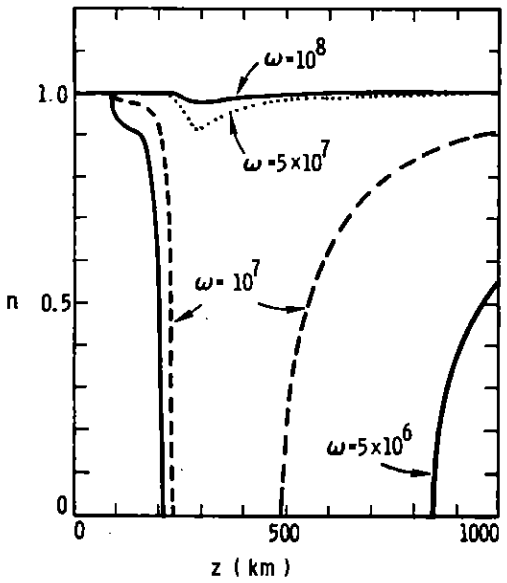

Figure 2. Index of Refraction of the Atmosphere as a Function of Altitude for Selected Frequencies

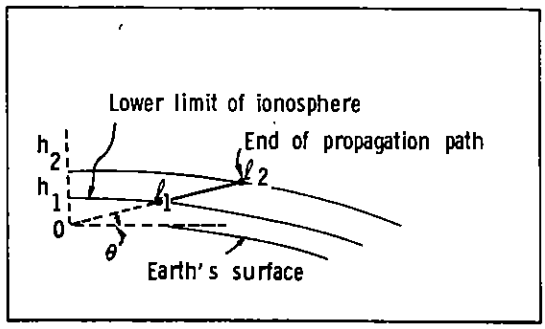

Figure 3. Geometry for Correction of TEC for Oblique Propagation

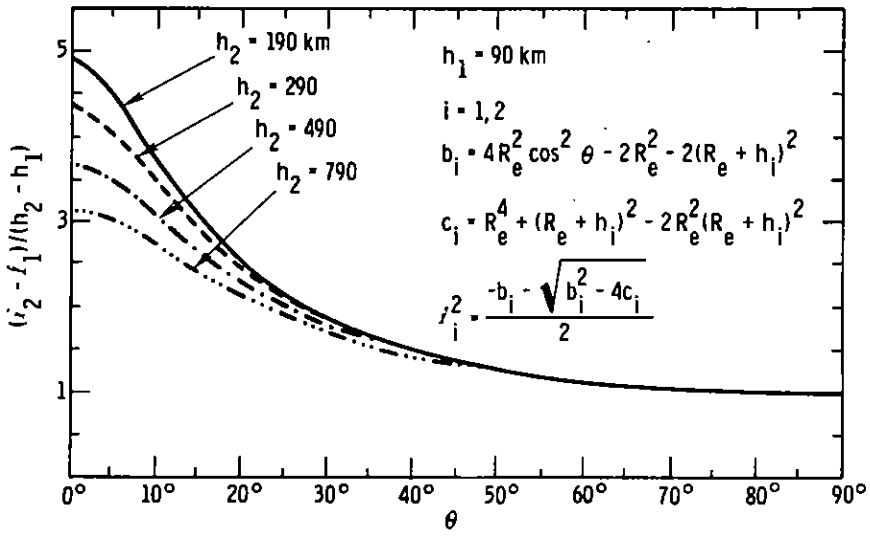

Figure 4. Geometrical Correction Factor for the TEC in the Case of Oblique Propagation Through the Ionosphere

Terms in the Series Expansion of the Transmitted-Pulse Phase Angle

The phase shift caused by propagation of the pulse through a material of index of refraction $n(\omega, z)$ is given by

$$\varphi = \frac{1}{c} \int_0^z \omega n(\omega, z')dz' , \tag{22}$$

where ω is in the range of validity of geometrical optics;[1] i.e.,

$$\frac{c}{\omega} \left| \frac{d(n \cos \theta)/dz}{n^2 \cos^2 \theta} \right| \ll 1 ,$$

with Snell's law, $n(z) \sin \theta(z) = \sin \theta_o$. This approach is valid for the propagating (nonreflected) waves.

The phase velocity is $v_p = c/n(\omega) = \omega/k'$ where k' is the wave number. The "pulse" is propagated at the group velocity $v_g = d\omega/dk' = c/[n(\omega) + \omega dn/d\omega]$. If z is the distance the pulse travels (group distance), the optical path length is given by

$$L_o = \int_0^z n(\omega, z)dz$$

$$= \int_0^z \frac{c}{v_p} dz \equiv c\Delta t_p ,$$

where Δt_p is the phase delay time. The group path length and group delay time are defined by

$$L_{gr} = \int_0^z \frac{c}{v_g} dz = c\Delta t_g .$$

When the pulse spreads in time, the shape varies with position and the group velocity must be interpreted with care.

Let us now return to the expansion of the phase angle given by Eq. (11). The frequency interest is confined to a series of narrow bands centered at $\omega = \omega_k$ for $k = 1, 2, \ldots K$. From Eq. (22), several factors in Eq. (11) are now evaluated. The phase shift at ω_k is

$$\varphi(\omega_k) = \frac{\omega_k}{c} \int_0^z n(\omega_k, z)dz = \frac{\omega_k}{c} L_o = \omega_k \Delta t_p , \tag{23}$$

and the group delay time becomes

$$\varphi'(\omega_k) = \frac{1}{c}\int_o^z \left[n(\omega,z) + \omega\frac{dn(\omega,z)}{d\omega}\right]_{\omega=\omega_k} dz .$$

Since n is given by Eq. (21), the delay simplifies to

$$\varphi'(\omega_k) = \frac{1}{c}\int_o^z n^{-1}(\omega_k,z)\,dz . \tag{24}$$

The dispersion at $\omega = \omega_k$ is given by

$$\varphi''(\omega_k) = \frac{d}{d\omega}\left[\varphi(\omega)\right]_{\omega=\omega_k} .$$

Again, by use of Eq. (21),

$$\varphi''(\omega_k) = \frac{1}{c}\int_o^z \frac{(n^2-1)\,dz}{\omega_k n^3} . \tag{25}$$

In a similar manner,

$$\varphi'''(\omega_k) = \frac{1}{c\omega_k^2}\int_o^z \left[\frac{n^4 - 4n^2 + 3}{n^5}\right] dz . \tag{26}$$

In a broad range of situations illustrated by Figure 2, the index of refraction is close to 1. In that case, from Eq. (21)

$$n \approx 1 - e^2N/2\epsilon_o m_e\omega^2 , \quad n^{-1} = 1 + e^2N/2\epsilon_o m_e\omega^2 ,$$

and with the definition $C_e = e^2TEC/2\epsilon_o m_e c$, Eqs. (23) through (26) become

$$\begin{aligned}
\varphi(\omega_k) &= \omega_k z/c - C_e/\omega_k , \\
\varphi'(\omega_k) &= z/c + C_e/\omega_k^2 , \\
\varphi''(\omega_k) &= -2C_e/\omega_k^3 , \\
\varphi'''(\omega_k) &= -4C_e/\omega_k^4 .
\end{aligned} \tag{27}$$

Note that the explicit z dependence of the phase is contained in the $\varphi(\omega_k)$ and $\varphi'(\omega_k)$ terms. The combined z dependence is $\omega z/c$, consistent with the propagation of a wave in the +z direction. If this z dependence is suppressed,

$$\varphi_s(\omega_k) = -C_e/\omega_k ,$$

$$\varphi_s'(\omega_k) = C_e/\omega_k^2 ,$$

$$\varphi''(\omega_k) = -2\varphi_s'(\omega_k)/\omega_k ,$$

$$\varphi'''(\omega_k) = 2\varphi''(\omega_k)/\omega_k .$$

The expansion becomes

$$\varphi(\omega) = \omega z/c - C_e/\omega_k + (\omega - \omega_k)\, C_e/\omega_k^2 - (\omega - \omega_k)^2\, C_e/\omega_k^3$$

$$- \frac{2}{3}(\omega - \omega_k)^3\, C_e/\omega_k^4 + \ldots .$$

For analysis in the frequency domain, Eq. (7) and Eq. (10) lead to

$$E(\omega) = \frac{1}{2\pi i} \sum_{k=0}^{K} c_k e^{i\varphi_k} \frac{\exp[i(\omega_k - \omega)T] - 1}{\omega_k - \omega} R(\omega) .$$

Under the present assumptions, $R(\omega) = e^{-i\varphi(\omega)}$, with the phase given as above. This representation of the transmitted pulse could be folded into a system response to determine a recorded signal. However, the results presented here are confined to the time domain.

Transmitted Pulse Form

Rather than continue the extension to higher order terms, one may now examine the relative size of the terms in order to obtain the simplest justifiable form for the transmitted pulse. Eq. (19) is valid (1) if $\omega_k T_k/\pi - u \gg 1$ in the range $-\vartheta_k/T_k \le u \le (T - \vartheta_k)/T_k$ and (2) if the φ''' and higher order terms are negligible. Recall that $T_k \sqrt{\pi |\varphi'''(\omega_k)|}$, $\vartheta_k = t - \varphi'(\omega_k)$, and T is the pulse duration. Thus, if ω_k is sufficiently large and ϑ_k and T are sufficiently small, use of Eq. (19) is reasonable. If, for Eq. (8), $N_1 = 1$, $T = 1\ \mu s$, $a = 4\ \mu s^{-1}$, $b = 476\ \mu s^{-1}$ are the incident-pulse parameter choices, then $\omega_k = 2\pi k$ rad/μs. The ratio of the φ''' term to the dispersion term in the phase is $\frac{2}{3}(\omega - \omega_k)/\omega_k$. Since Eq. (7) indicates that the incident pulse contributes only for each $\omega \approx \omega_k$, the ratio is small when the k^{th} component contributes to the transmitted pulse. This same $\Delta\omega/\omega_k$ term appears in higher powers for the ratio of higher order terms to the dispersion term. Hence, neglect of higher order terms is justified. The other requirement of Eq. (19) is that

$$\frac{\omega_k |\varphi''|}{T_k} - u \gg 1 .$$

The largest value that u can become is $(T - \theta_k)/T_k$. Since θ_k measures time after the leading edge of that frequency component starts contributing to the observed pulse, the largest u is T/T_k. Hence, the requirement may be written

$$\omega_k T_k/\pi >> 1 + T/T_k .$$

Since $C_e = e^2(TEC)/2\epsilon_o m_e c = 5.3042 \times 10^{-6} m^2/s \times TEC$, Eq. (27) indicates that $\omega_k T_k/\pi = [2C_e/(\pi\omega_k)]^{1/2}$ can be large only for restricted values of TEC. The term is unity at TEC = $\pi\omega_k \times 10^{12}/(10.6\ m^2/\mu s)$. Thus, for TEC (electrons/m^2) $> 10^{12} \times \omega_k$(rad/$\mu$s) the $\omega_k T_k/\pi$ is large, as required. The ω_k of interest ranges from 1 to $\gtrsim$ 20 times 20 rad/μs; hence, the lower limit for TEC is TEC $\geq 5 \times 10^{14}$ electrons/m^2. At TEC = 5×10^{14} electrons/m^2 and ω_k = 20 rad/μs, then T_k = 1.4 μs and the requirements of Eq. (19) are easily satisfied. With ω_k increased by a factor of 10, however, the requirement on T_k fails unless the TEC is increased by a factor approximately equal to 100. Since 10 terms may be necessary in the pulse expansion, at least as a check upon a sufficient number of terms being present, Eq. (19) does not have sufficient generality for calculating the transmitted pulse. The equation is not adequate to describe strong spreading of short pulses.

Large dispersion is sometimes[3] quantified by $|\varphi''| >> 1/(\Delta\omega)^2$, where $\Delta\omega$ is the band pass being received or propagated. This is equivalent to $\omega_k T_k/\pi >> \omega_k/(\sqrt{\pi}\,\Delta\omega)$. For the k^{th} component of the quasi-monochromatic wave, the $\Delta\omega \approx \omega_k$. Hence, a restriction of large dispersion is consistent with the restriction for validity of Eq. 19 (the T/T_k is then a ratio of the order of 1) for each individual frequency component. It has been noted that at higher frequencies Eq. (19) is no longer valid. This is consistent with failure of the large-dispersion approximation. For TEC = 2.5×10^{16} electrons/m^2, large dispersion is questionable for $k \gtrsim 40$. With the present choice T = 1 μs, $\omega_k = 2\pi$ k rad/μs; hence, the index of refraction ≈ 1 for $k \geq 10$. The k = 10 component arrives > 30 μs after the k = 40 component; hence, the approximation $\omega_p \ll \omega$ is valid for the first 30 μs of the calculated signal if $K \geq 40$ and if TEC = 2.5×10^{16} electrons/m^2.

In the present case, where the incident signal is a series of quasi-monochromatic pulses, large dispersion requires the propagated signal to be a sequence of dispersed pulses. If the dispersed pulse duration is greater than the time between pulse arrivals, the pulses interfere to form quite complicated waveforms. For increased generality, one may now consider Eq. (18). Here, it is assumed that φ''' and higher order terms may be disregarded, with no restriction on the dispersion.

$$E_{a3}(t) = \sum_{k=1}^{K} \frac{c_k e^{i\varphi_k}}{2} \exp\left[i\left(\omega_k t - \varphi(\omega_k)\right)\right] \times I_k , \qquad (28)$$

where

$$I_k = \int_{-\theta_k/T_k}^{(T-\theta_k)/T_k} \exp\left(\frac{i\pi u^2}{2}\right)\left[\frac{1-i}{2} - F^*(\xi_1)\right] du \tag{29}$$

and $\xi_1 = u - \omega_k T_k/\pi$. Since relative values of TEC and ω_k are not restricted, this form is justified for the ionosphere and the pulse models chosen for cases when K is extended to larger numbers.

The integration limits span the time the pulse can contribute to E(t), with corrections for the delay of various frequency components. The delay is $\omega' = z/c + C_e/\omega_k^2$. As expected, the higher frequency components are propagated with the least delay. The phase angle for the carrier wave is $\omega_k(t - z/c) + C_e/\omega_k$. The $e^{i\varphi_k}$ could be considered as adding an angle to the carrier phase; φ_k does not affect the delay of the k^{th} frequency component of the signal.

In evaluation of Eq. (28) ξ_1 is often < -10; therefore, $F^*(\xi_1) \approx -(1 - i)/2$. Hence, in order to increase efficiency, the integral in Eq. (29) may be written as

$$I_k = (1 - i)\left[F\left(\frac{T - \theta_k}{T_k}\right) + F\left(\frac{\theta_k}{T_k}\right)\right] - \int_{-\theta_k/T_k}^{(T-\theta_k)/T_k} \exp\left(\frac{i\pi u^2}{2}\right)\left[C(\xi_1) + \frac{1}{2} - iS(\xi_1) - \frac{i}{2}\right] du . \tag{30}$$

For many cases, the integral in Eq. (30) represents a small correction term. The auxiliary functions

$$f(z) = \left[\frac{1}{2} - S(z)\right] \cos\frac{\pi z^2}{2} - \left[\frac{1}{2} - C(z)\right] \sin\frac{\pi z^2}{2} , \tag{31}$$

$$g(z) = \left[\frac{1}{2} - C(z)\right] \cos\frac{\pi z^2}{2} + \left[\frac{1}{2} - S(z)\right] \sin\frac{\pi z^2}{2} , \tag{32}$$

with

$$a_k = \omega_k T_k/\pi ,$$

$$y_1 = a_k - \frac{T - \theta_k}{T_k} ,$$

$$y_2 = a_k + \frac{\theta_k}{T_k} ,$$

$$p_{1,2} = \pi a_k y_{1,2} - \frac{\pi a_k^2}{2} ,$$

allow I_k to be written

$$I_k = (1 - i)\left[F\left(\frac{T - \theta_k}{T_k}\right) + \left(F\ \frac{\theta_k}{T_k}\right)\right]$$

$$+ \int_{p_1}^{p_2} [f(y)(\sin p + i \cos p) - g(y)(\cos p - i \sin p)] \frac{dp}{\pi a_k}, \tag{33}$$

where $y = (p + \pi a_k^2/2)/(\pi a_k)$. The SICONT subroutine[8] is used for evaluating the correction term. The methods used to calculate the Fresnel integrals and the auxiliary functions are given in Appendix A.

In certain situations the ξ_1 of Eq. (29) becomes large and positive. Since the correction term can be significant in such cases, the form of Eq. (33) gives difficulty because of the rapidly fluctuating f and g when their arguments are negative. One is forced back to the earlier form

$$I_k = \int_{-\theta_k/T_k}^{\beta_k} \exp\left(\frac{i\pi u^2}{2}\right)\left[\frac{1-i}{2} - F^*(u-a_k)\right] du, \tag{34}$$

with $\beta_k \equiv (T-\theta_k)/T_k$. Let I_- denote the portion of I_k contributed by $u \le a_k$. With $u_\ell \equiv$ the smaller of a_k and β_k, with $\beta_k > 0$, and with the definition

$$\mathcal{F}(\alpha, \beta) \equiv (1-i)[F(\alpha) + F(\beta)], \tag{35}$$

one finds

$$I_- = \mathcal{F}\left(u_\ell, \frac{\theta_k}{T_k}\right) + \frac{w}{\pi a_k} \int_{z_1}^{z_2} \left\{g[\nu_k(z)]\ e^{-iwz} - if[\nu_k(z)]\ e^{-iwz}\right\} dz, \tag{36}$$

where $\nu_k(z) = a_k/2 + wz/(\pi a_k)$ and w is a constant chosen as the largest of the three values 1, $|\mu_\ell|$, and θ_k/T_k. The limits of integration are $z_1 = w^{-1}(\pi\ a_k^2/2 + \pi\ a_k\ \theta_k/T_k)$ and $z_2 = w^{-1}(\pi a_k^2/2 - \pi a_k\ u_\ell)$. In this form the $\nu_k \ge 0$; hence, the f and g are well behaved, and the numerical integration is straightforward by use of the SICONT subroutine.[8]

If $u_\ell = \beta_k$, then $I_k = I_-$ and evaluation is complete. If the restriction $\beta_k > 0$ is removed, then the integral in Eq. (34) is over a region of negative u. Again, with $u_\ell = \beta_k$ (as it would be for $\beta_k < 0$), one has $I_k = I_-$. However, if $u_\ell = a_k$, then $I_k = I_- + I_+$, where

$$I_+ = \int_{a_k}^{\beta_k} \exp\left(\frac{i\pi u^2}{2}\right)\left[\frac{1-i}{2} - F^*(u-a_k)\right] du.$$

Again, to take advantage of the design of the SICONT routine for integration of rapidly oscillating functions, let w be the larger of 1 and β_k. Then the integral may be written.

$$I_+ = \frac{w}{\pi a_k} \int_{z_1'}^{z_2'} \left\{ g[\nu_k'(z)]\, e^{iwz} - if[\nu_k'(z)]\, e^{iwz} \right\} dz, \tag{37}$$

where

$$\nu_k'(z) = \frac{wz}{\pi a_k} - \frac{a_k}{2}, \quad z_1' = \frac{\pi a_k^2}{2w}, \text{ and } z_2' = \frac{\pi a_k \beta_k - \pi a_k^2/2}{w} .$$

In summary, $I_k = I_-$ for $u_\ell = \beta_k$; $I_k = I_- + I_+$ for $u_\ell = a_k$. The field is evaluated from Eq. (28), with I_k given by Eqs. (33)-(37).

Results for TEC = 2.5×10^{16} Electrons/m^2

Before presenting results, one first checks the earlier assumption that $n \approx 1$. The delay is $\varphi_s'(\omega_k) = C_e/\omega_k^2 = \omega_p^2\, TEC/(2cN\, \omega_k^2)$. When $\omega_k = \omega_p$, the index of refraction becomes zero, and propagation of that component ceases. Figure 5 illustrates the plasma frequency in the model ionosphere as well as the delay, δ, required by the constraint that the index of refraction become zero. Hence, for TEC as low as 10^{13} electrons/m^2 ($z \approx 100$ km) and with $n \approx 1$ assumed, the first ~ 10 μs of signal may be evaluated. At an altitude of 350 km (TEC $\approx 10^{16}$ electrons/m^2) and with $n \approx 1$ assumed, the first 300 μs of propagated signal may be evaluated. For oblique paths through the ionosphere, the times are increased further. Of course, with these delays it is assumed that the incident pulse has frequency components sufficiently high for the contributions to occur after existing, higher frequency contributions. The lower frequency terms that arrive after these delays will experience small indices of refraction and suffer significant attenuation that is not taken into account in the present model.

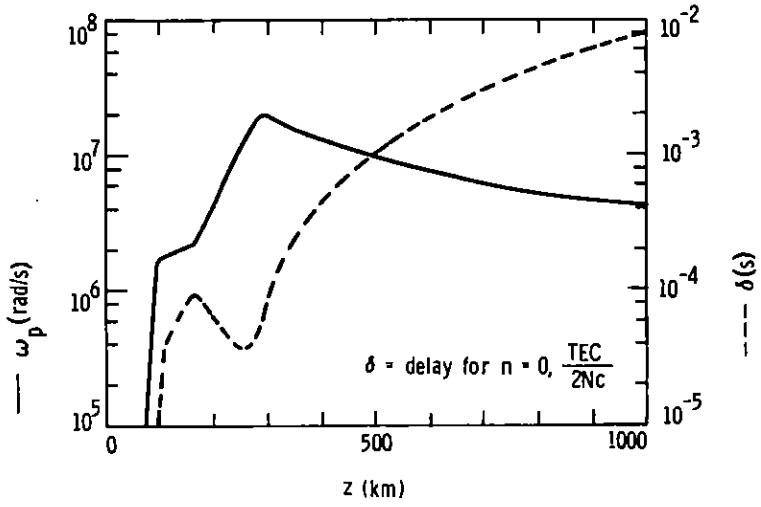

Figure 5. Plasma Frequency and δ (i.e., TEC/2Nc)) for a Vertically Upward Path Through the Model Ionosphere

With the parameter choices given at the beginning of the foregoing section, the double exponential and the approximation of Eq. (1) are represented in Figure 6. The c_k and φ_k of Eqs. (9) are illustrated in Figure 7. The c_k indicates that frequency components exist up to quite high frequencies, as indicated in Figure 8. It is assumed that wavelengths less than 2 m are to be neglected in the incident pulse. This might correspond to the interaction of the electromagnetic pulse with an antenna a few meters long for which the response would be negligible for wavelengths $\lambda < 2$ m.[9] With the choice T = 1 μs, then K = 150 includes all components which effectively contribute to the response of such an antenna. The results presented have used K = 325 and are very similar to the K = 150 results. The observed wave is then given in Figure 9 (recall that the incident wave is unitless, with peak value 0.93). The delay, φ_s', suffered by each frequency component is shown in Figure 10. Comparison of these two figures at later times allows one to identify the k corresponding to the arrival of some of the low-frequency components. The summation in Eq. (28) omits those components for which $\theta_k < 0$, since they have not had sufficient time to arrive at the observation point. The pulses, however, are quasi-monochromatic with width $\Delta\omega \approx \omega_k$. From Eq. (7) the k^{th} component of $g(\omega)$ reaches zero when $\omega = 2\ \omega_k$. In these results each component is assumed to start contributing after the θ_k corresponding to $2 \times \omega_k$ passes zero. For consistency, the delay in Figure 10 for each component, k, was calculated for $\omega = 2 \times \omega_k$. This alteration of θ_k increased the peak value of the transmitted signal by a factor near 2 and caused more rapid decay of amplitude with time for TEC = 2.5×10^{16} electrons/m^2.

If Eqs. (28) and (29) were applied to the case of very low dispersion, one might expect the equations to give a reasonable approximation to the incident pulse. The T_k being small would result in large correction terms. In that case, however, the proper procedure would be to neglect the dispersion term as in Eq. (15).

The fraction by which the ionosphere has reduced $|E(t)|_{max}$ can be found in Figures 6 and 9. For the TEC value 2.5×10^{16} electrons/m^2, the fraction, f, is 0.077. The series of transmitted pulses given in Appendix B allows evaluation of this fraction for a range of TEC values. Figure 11 compares these results, which allow constructive interference of frequency components, with data, given by Messier, based upon high dispersion.[2] In order to facilitate this comparison, the choices of a and b for the double exponential match those used by Messier for his incident double exponential. The higher values of f presented here indicate that the high-frequency, low-dispersion components add constructively to produce the maximum amplitude in the transmitted signal.

Conclusions

In a review of theory for the dispersion of electromagnetic pulses propagating through the ionosphere, correction terms found allowed extension of the theory to the case where dispersion, although not large, is not negligible. The pulse chosen for illustration had a dispersed-pulse duration greater than the time between arrivals of the various frequency components. The components interfere to form quite complicated waveforms. The high-frequency, relatively low-dispersion components were found to add constructively to produce the maximum amplitude in the transmitted signal. This amplitude was significantly affected by the inclusion of the correction terms.

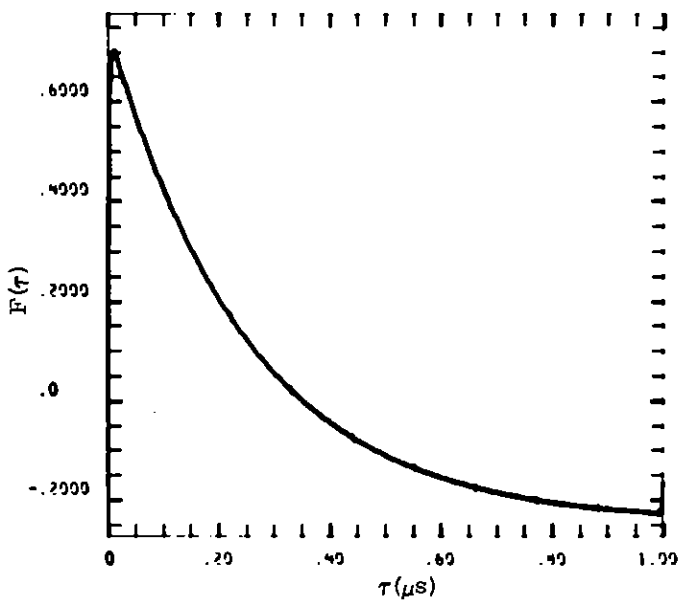

A= 4.0
B= 476.0
T= 1.0
K= 325.0
TEC = 1.0E+00
PEAK N 1.0E+00
ω CUT 0.

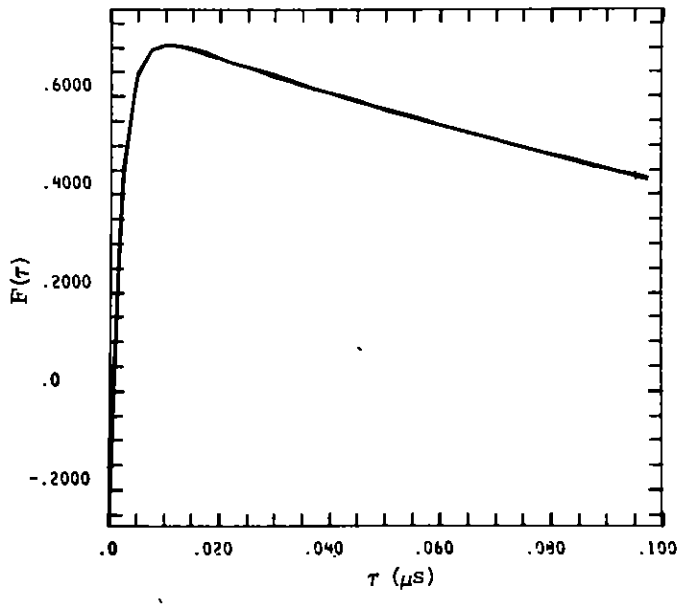

A= 4.0
B= 476.0
T= 1.0
K= 325.0
TEC = 1.0E+00
PEAK N 1.0E+00
ω CUT 0.

Figure 6. Incident Double-Exponential Pulse and Its Series Representation, After Subtraction of the dc (c_o) Component

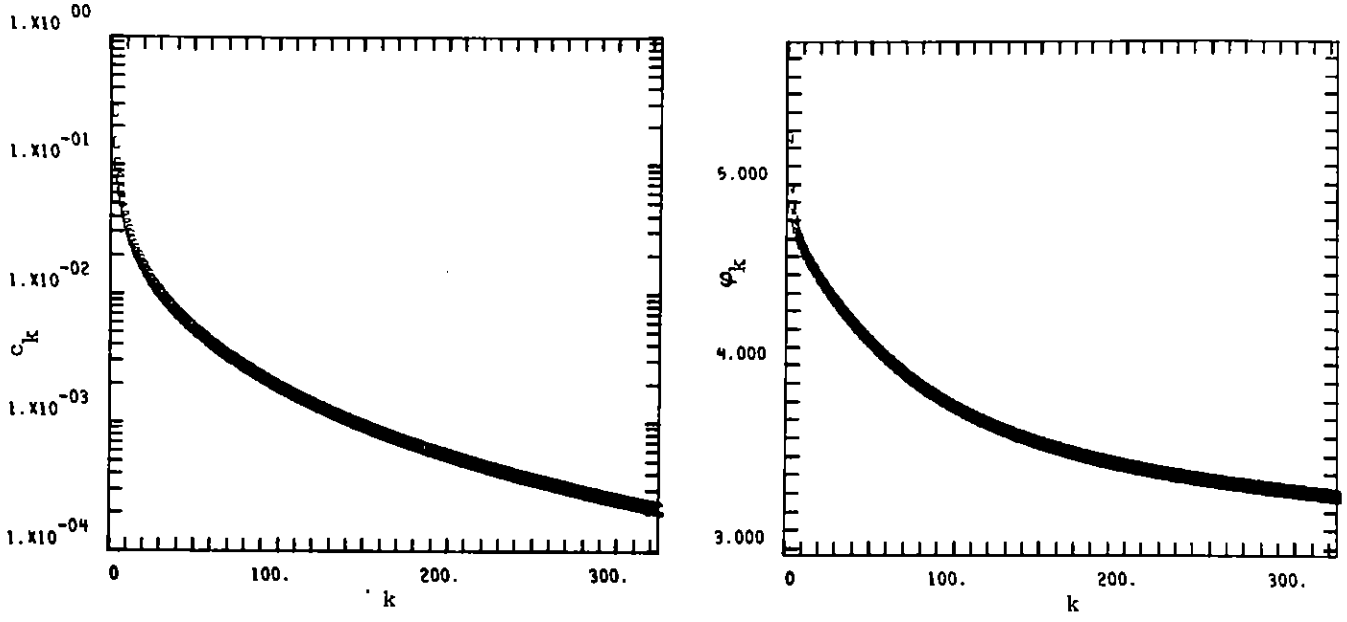

Figure 7. c_k and φ_k (radians) Tabulated as Functions of k

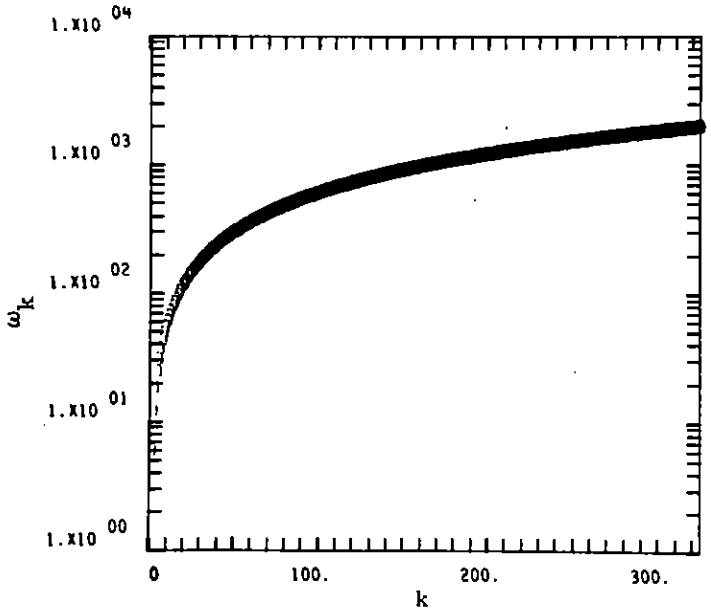

Figure 8. Angular Frequency ω_k Tabulated as a Function of k

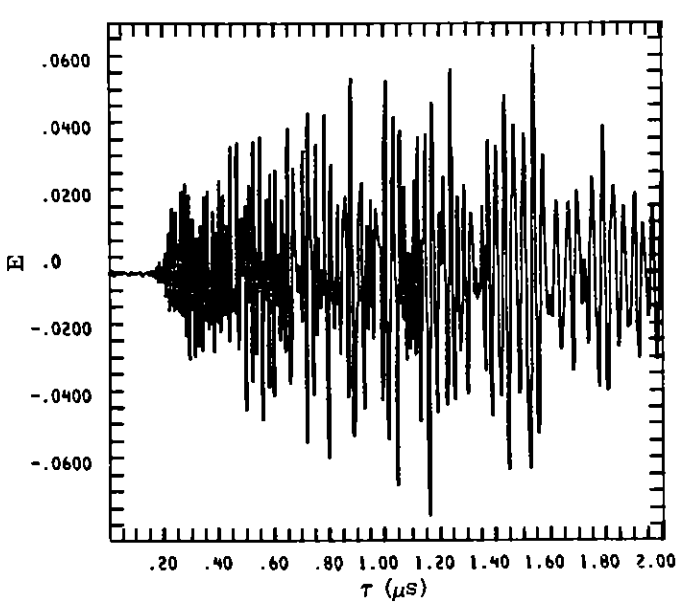

A= 4.0
B= 476.0
T= 1.0
K= 325.0
TEC = 2.5E+16
PEAK N 1.3E+11
ω CUT 2.1E+01

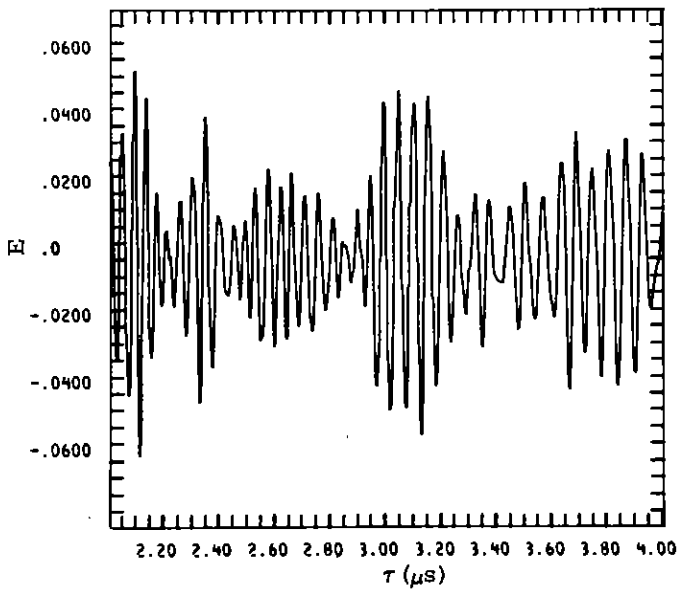

A= 4.0
B= 476.0
T= 1.0
K= 325.0
TEC = 2.5E+16
PEAK N 1.3E+11
ω CUT 2.1E+01

Figure 9. Transmitted Pulse up to 8 μs

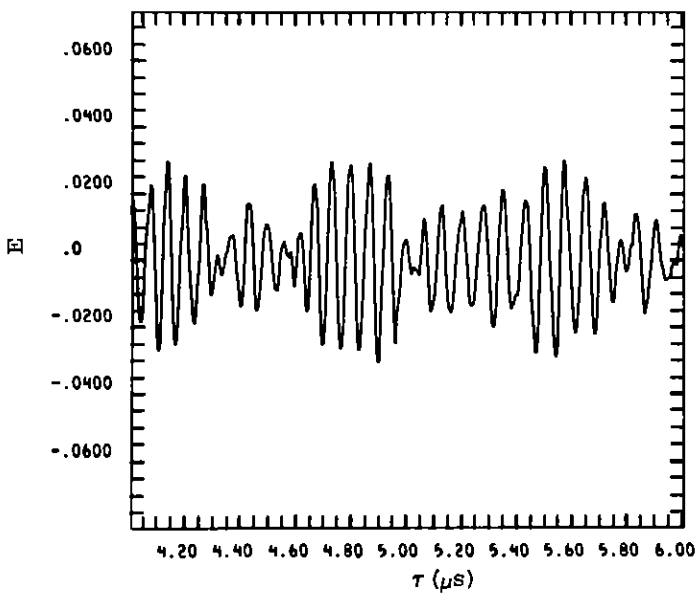

A= 4.0
B= 476.0
T= 1.0
K= 325.0
TEC = 2.5E+16
PEAK N 1.3E+11
ω CUT 2.1E+01

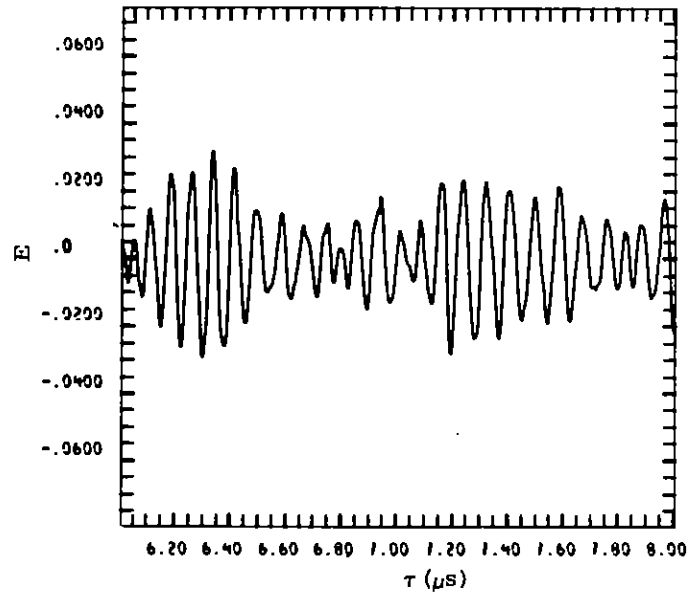

A= 4.0
B= 476.0
T= 1.0
K= 325.0
TEC = 2.5E+16
PEAK N 1.3E+11
ω CUT 2.1E+01

Figure 9 (cont)

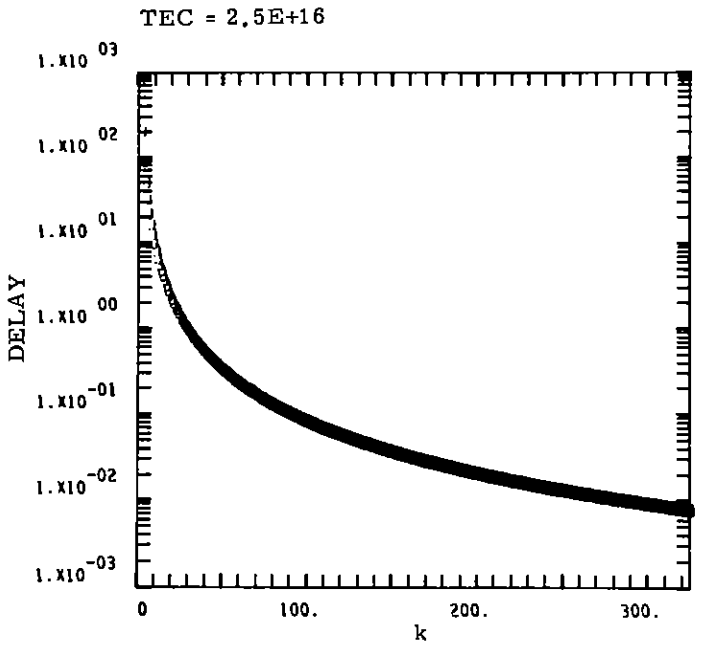

Figure 10. Delay (φ_s' (2 ω_k) in μs) for TEC = 2.5E16 Electrons/m^2 Tabulated as a Function of k

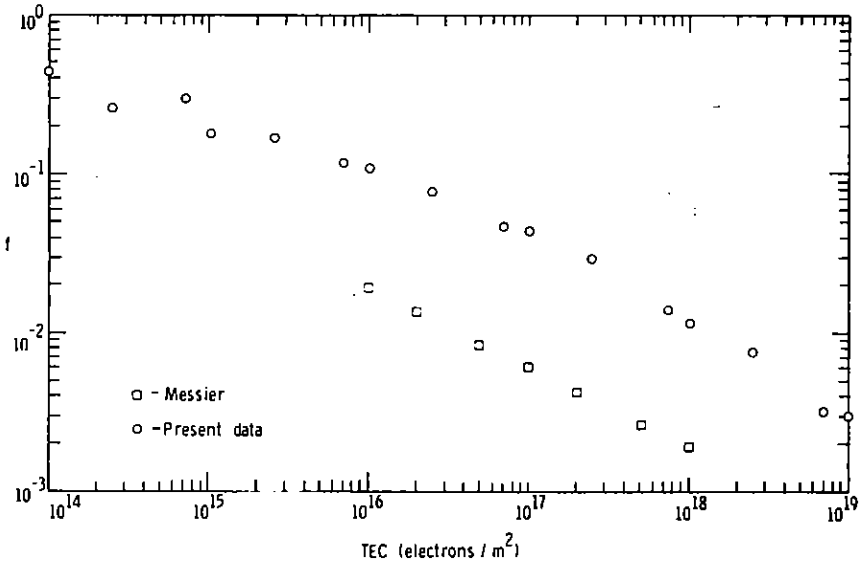

Figure 11. Ionospheric Amplitude Reduction Factor for Selected TEC Values

Appendix A

COMPUTATION OF FRESNEL INTEGRALS AND AUXILIARY FUNCTIONS

A transformation of variables allows one to take advantage of Boersma's* work for evaluating the Fresnel integral. The maximum error is quoted as 1.6×10^{-9}. For $\pi x^2/2 \geq 4$, the results are

$$f(x) = \sqrt{\frac{8}{\pi x^2}} \sum_{n=0}^{11} d_n \left(\frac{8}{\pi x^2}\right)^n ,$$

$$g(x) = -\sqrt{\frac{8}{\pi x^2}} \sum_{n=1}^{11} c_n \left(\frac{8}{\pi x^2}\right)^n ,$$

$$C(x) = \frac{1}{2} - g(x) \cos \frac{\pi x^2}{2} + f(x) \sin \frac{\pi x^2}{2} ,$$

$$S(x) = \frac{1}{2} - g(x) \sin \frac{\pi x^2}{2} - f(x) \cos \frac{\pi x^2}{2} .$$

This restricted region of x is the one most often encountered. For large x, the f(x) and g(x) become small.

In the region $0 \leq \pi x^2/2 \leq 4$, the results are

$$f(x) = \sqrt{\frac{\pi x^2}{8}} \sum_{n=0}^{11} b_n \left(\frac{\pi x^2}{8}\right)^n + \frac{1}{2}\left\{\cos \frac{\pi x^2}{2} - \sin \frac{\pi x^2}{2}\right\} ,$$

$$g(x) = \sqrt{\frac{\pi x^2}{8}} \sum_{n=0}^{11} -a_n \left(\frac{\pi x^2}{8}\right)^n + \frac{1}{2}\left\{\cos \frac{\pi x^2}{2} + \sin \frac{\pi x^2}{2}\right\} ,$$

$$C(x) = \sqrt{\frac{\pi x^2}{8}} \sum_{n=0}^{11} \left(\frac{\pi x^2}{8}\right)^n \left\{a_n \cos \frac{\pi x^2}{2} - b_n \sin \frac{\pi x^2}{2}\right\}.$$

and

$$-S(x) = \sqrt{\frac{\pi x^2}{8}} \sum_{n=0}^{11} \left(\frac{\pi x^2}{8}\right)^n \left\{b_n \cos \frac{\pi x^2}{2} - a_n \sin \frac{\pi x^2}{2}\right\}.$$

The coefficients are given in Table A-I.

*J. Boersma, "Computation of Fresnel Integrals," Math. Comp. 14, 380 (1960).

For the case of negative argument the following relations allow evaluation of the functions.

$$C(-x) = -C(x),$$

$$S(-x) = -S(x),$$

$$f(-x) = -f(x) + \cos \frac{\pi x^2}{2} - \sin \frac{\pi x^2}{2},$$

$$g(-x) = -g(x) + \cos \frac{\pi x^2}{2} + \sin \frac{\pi x^2}{2}.$$

TABLE A-I

Coefficients

i	a_i	b_i	c_i	d_i
0	+1.595769140	-0.000000033	0	+0.199471140
1	-0.000001702	+4.255387524	-0.024933975	+0.000000023
2	-6.808568854	-0.000092810	+0.000003936	-0.009351341
3	-0.000576361	-7.780020400	+0.005770956	+0.000023006
4	+6.920691902	-0.009520895	+0.000689892	+0.004851466
5	-0.016898657	+5.075161298	-0.009497136	+0.001903218
6	-3.050485660	-0.138341947	+0.011948809	-0.017122914
7	-0.075752419	-1.363729124	-0.006748873	+0.029064067
8	+0.850663781	-0.403349276	+0.000246420	-0.027928955
9	-0.025639041	+0.702222016	+0.002102967	+0.016497308
10	-0.150230960	-0.216195929	-0.001217930	-0.005598515
11	+0.034404779	+0.019547031	+0.000233939	+0.000838386

Appendix B

A SERIES OF PROPAGATED PULSES

A double-exponential pulse characterized by the parameters $N_1 = 1$, $T = 1\ \mu s$, $a = 4\ \mu s^{-1}$, and $b = 476\ \mu s^{-1}$ is assumed to be incident upon a series of TEC values. The incident pulse and associated constants are as described earlier in Figures 6-8. This appendix presents the resulting series of transmitted waves corresponding to Figure 9 for the TEC value 2.5×10^{16} electrons/m^2. The K value 325 was used for the calculations presented here. Comparison with results for K = 150 indicates that the latter number of terms would have been sufficient. Starting with the TEC = 1×10^{16} waveform, the results are presented for an additional 2-μs time because of their more complicated behavior. With TEC = 1×10^{18} and following graphs, each graph spans 1 μs rather than the 2 μs spanned in preceding graphs. Some unfortunate scale choices have been made. In the results for TEC = 7.0×10^{18} electrons/m^2, for example, the pulse should be slightly off scale (rather than discontinuous) near $\tau = 3.8\ \mu s$.

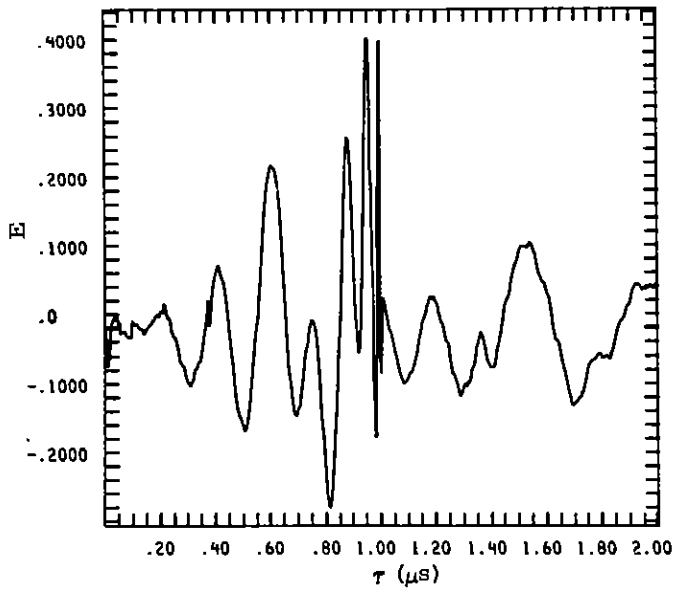

A= 4.0
B= 476.0
T= 1.0
K= 325.0
TEC = 1.0E+14
PEAK N 1.6E+09
ω CUT 2.3E+00

B-1a

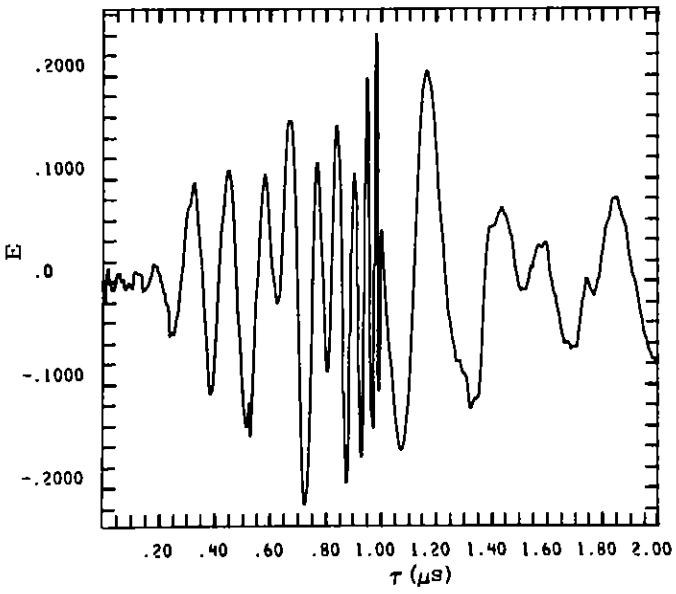

A= 4.0
B= 476.0
T= 1.0
K= 325.0
TEC = 2.5E+14
PEAK N 8.2E+09
ω CUT 5.1E+00

B-1b

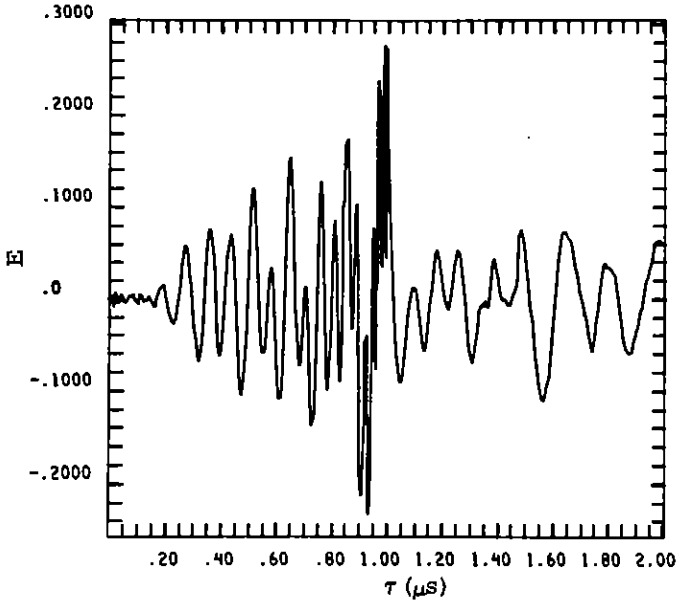

A= 4.0
B= 476.0
T= 1.0
K= 325.0
TEC = 7.0E+14
PEAK N 2.6E+10
ω CUT 9.0E+00

B-2a

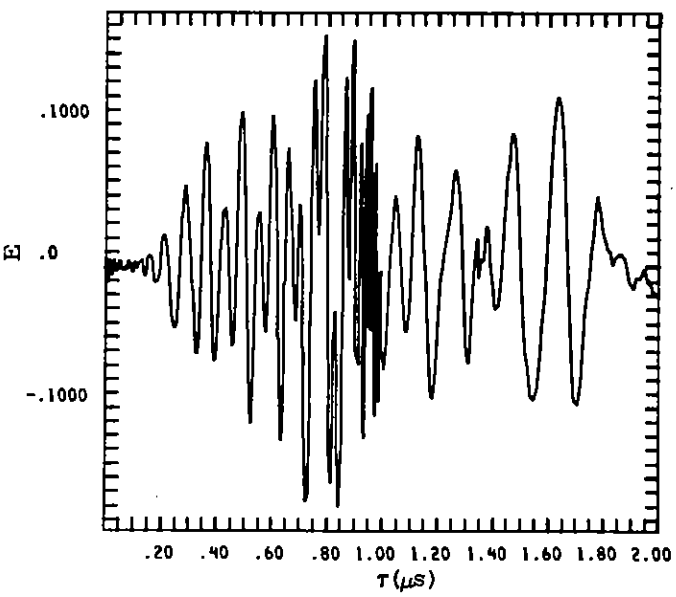

A= 4.0
B= 476.0
T= 1.0
K= 325.0
TEC = 1.0E+15
PEAK N 4.0E+10
ω CUT 1.1E+01

B-2b

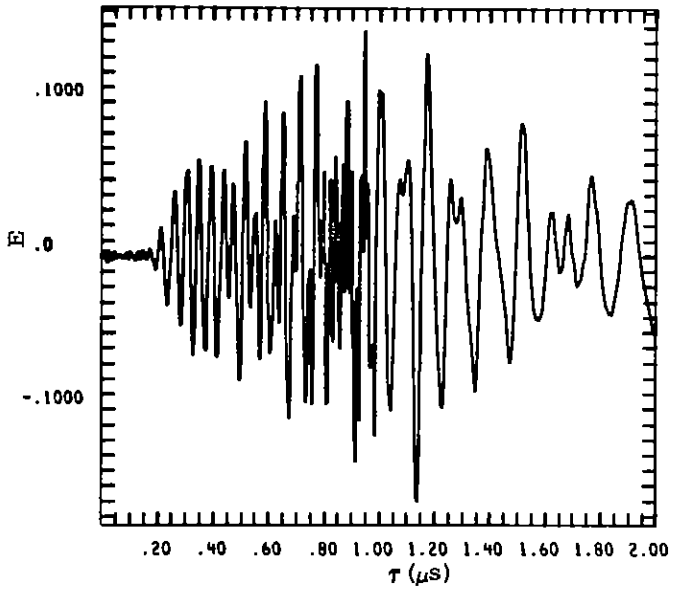

A= 4.0
B= 476.0
T= 1.0
K= 325.0
TEC = 2.5E+15
PEAK N 9.2E+10
ω CUT 1.7E+01

B-3a

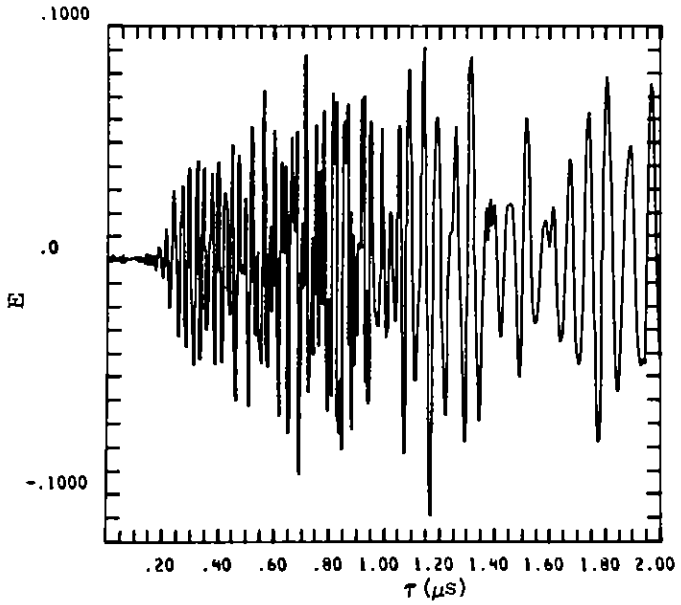

A= 4.0
B= 476.0
T= 1.0
K= 325.0
TEC = 7.0E+15
PEAK N 1.3E+11
ω CUT 2.1E+01

B-3b

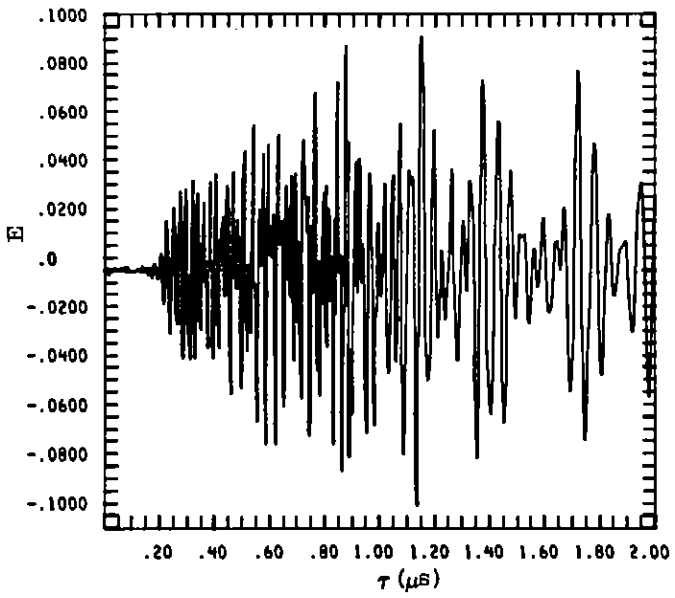

A= 4.0
B= 476.0
T= 1.0
K= 325.0
TEC = 1.0E+16
PEAK N 1.3E+11
ω CUT 2.1E+01

B-4a

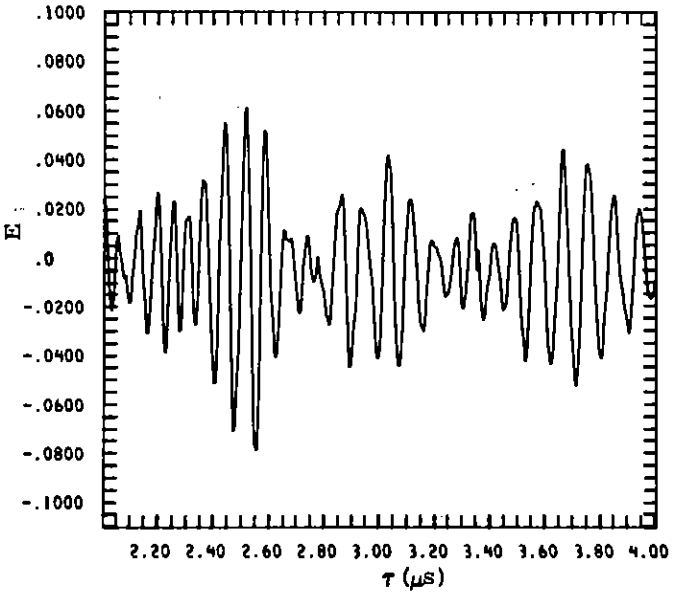

A= 4.0
B= 476.0
T= 1.0
K= 325.0
TEC = 1.0E+16
PEAK N 1.3E+11
ω CUT 2.1E+01

B-4b

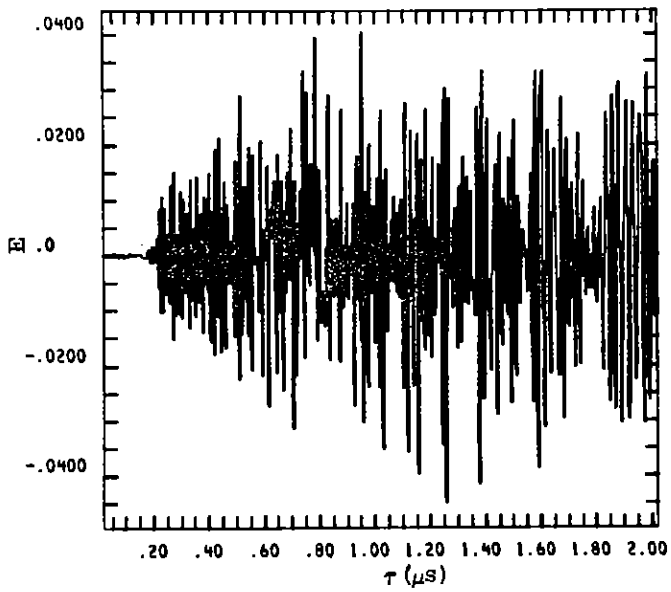

A= 4.0
B= 476.0
T= 1.0
K= 325.0
TEC = 7.0E+16
PEAK N 1.3E+11
ω CUT 2.1E+01

B-5a

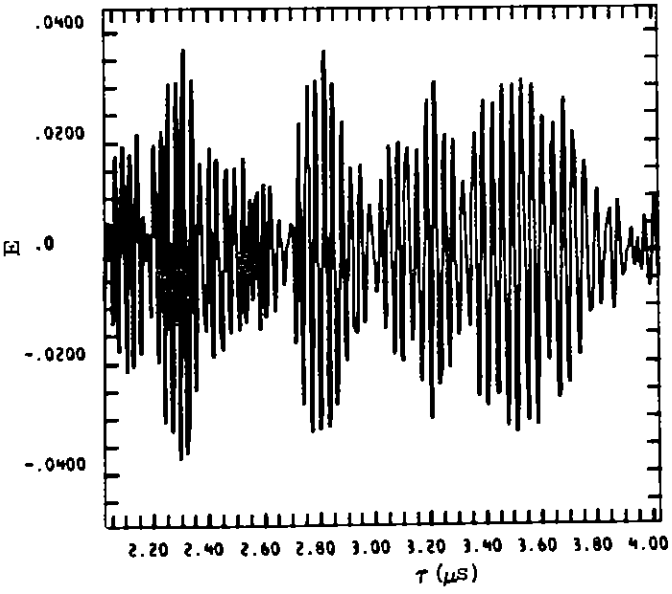

A= 4.0
B= 476.0
T= 1.0
K= 325.0
TEC = 7.0E+16
PEAK N 1.3E+11
ω CUT 2.1E+01

B-5b

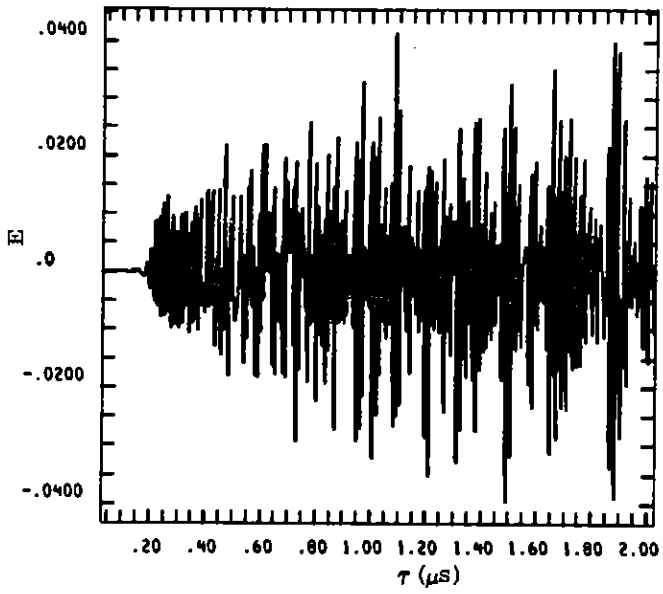

A= 4.0
B= 476.0
T= 1.0
K= 325.0
TEC = 1.0E+17
PEAK N 1.3E+11
ω CUT 2.1E+01

B-6a

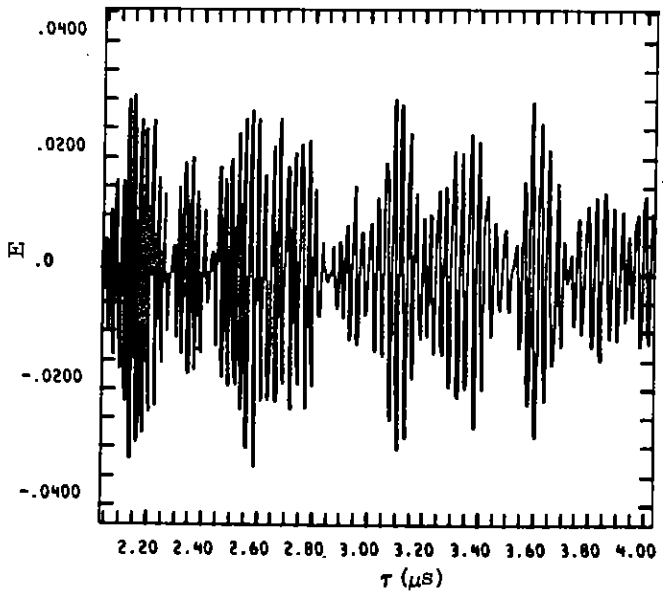

A= 4.0
B= 476.0
T= 1.0
K= 325.0
TEC = 1.0E+17
PEAK N 1.3E+11
ω CUT 2.1E+01

B-6b

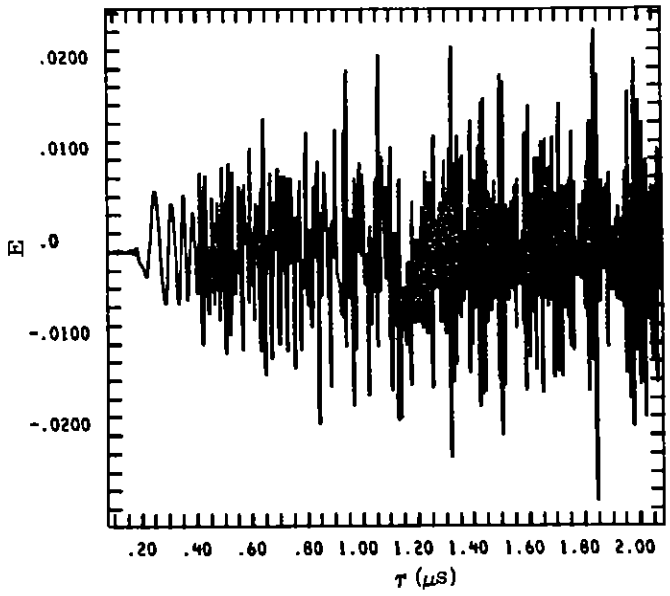

A= 4.0
B= 476.0
T= 1.0
K= 325.0
TEC = 2.5E+17
PEAK N 1.3E+11
ω CUT 2.1E+01

B-7a

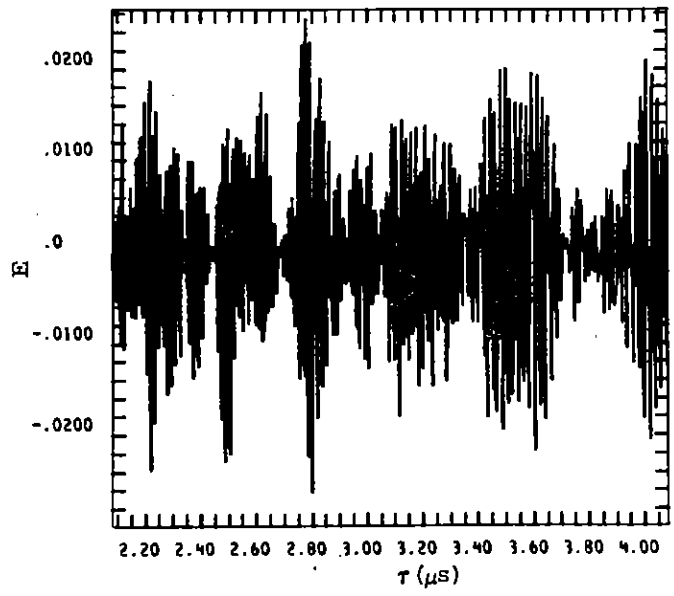

A= 4.0
B= 476.0
T= 1.0
K= 325.0
TEC = 2.5E+17
PEAK N 1.3E+11
ω CUT 2.1E+01

B-7b

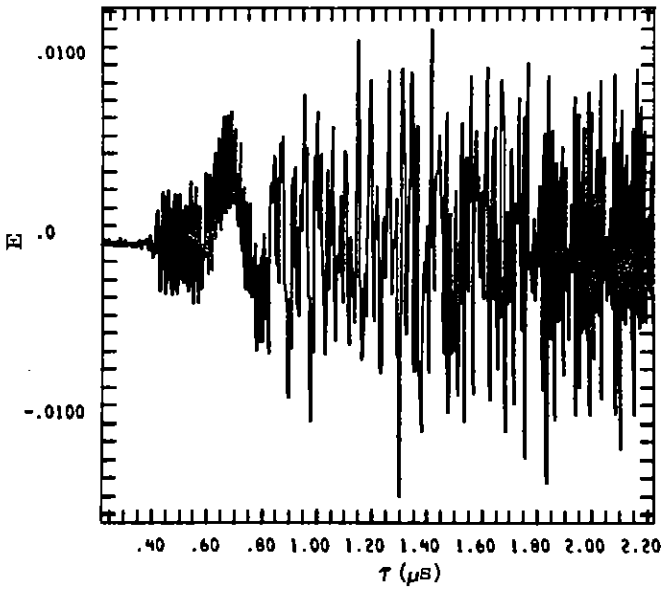

A= 4.0
B= 476.0
T= 1.0
K= 325.0
TEC = 7.0E+17
PEAK N 1.3E+11
ω CUT 2.1E+01

B-8a

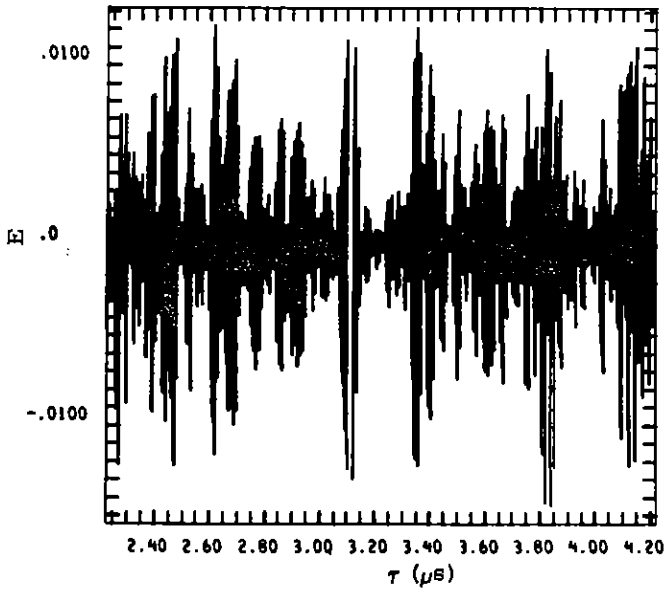

A= 4.0
B= 476.0
T= 1.0
K= 325.0
TEC = 7.0E+17
PEAK N 1.3E+11
ω CUT 2.1E+01

B-8b

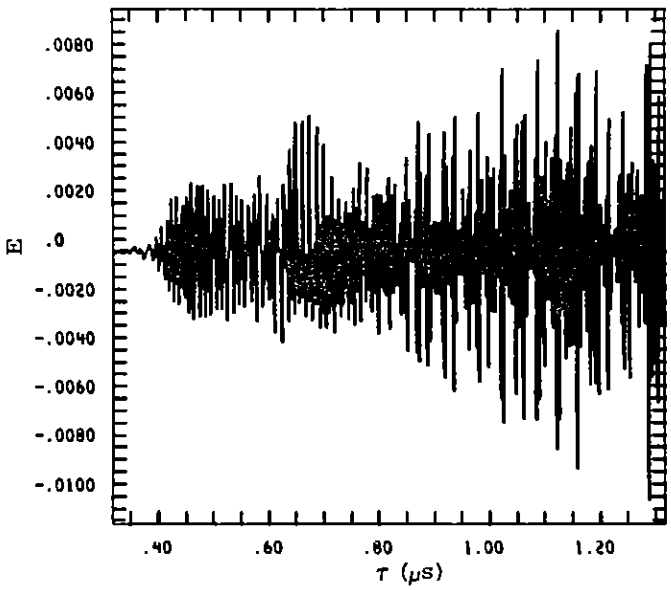

A= 4.0
B= 476.0
T= 1.0
K= 325.0
TEC = 1.0E+18
PEAK N 1.3E+11
ω CUT 2.1E+01

B-9a

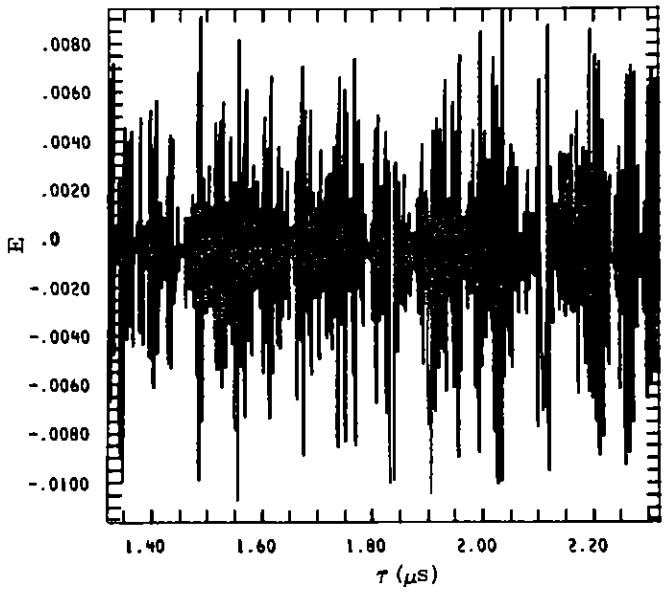

A= 4.0
B= 476.0
T= 1.0
K= 325.0
TEC = 1.0E+18
PEAK N 1.3E+11
ω CUT 2.1E+01

B-9b

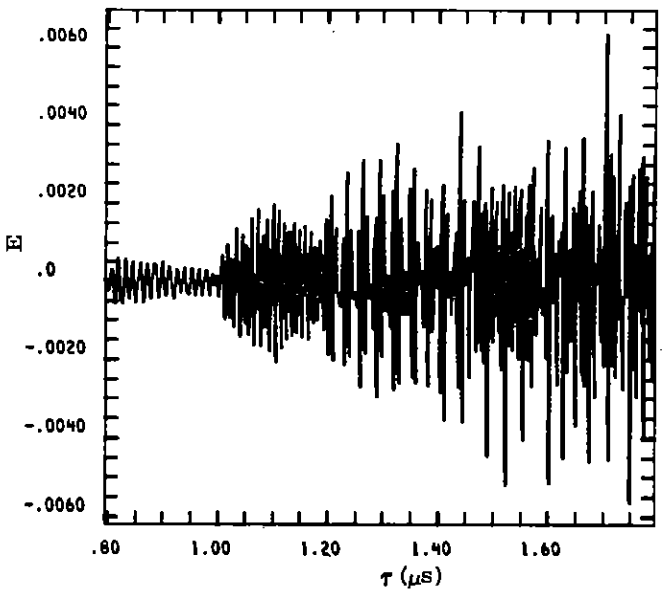

A= 4.0
B= 476.0
T= 1.0
K= 325.0
TEC = 2.5E+18
PEAK N 1.3E+11
ω CUT 2.1E+01

B-10a

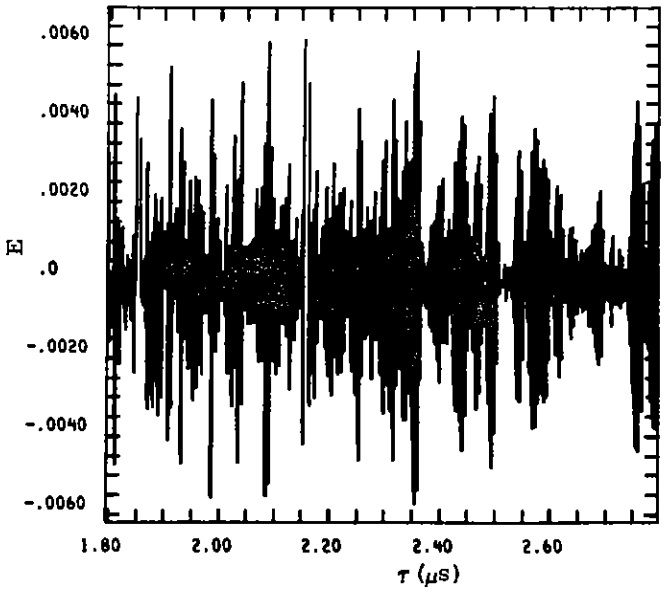

A= 4.0
B= 476.0
T= 1.0
K= 325.0
TEC = 2.5E+18
PEAK N 1.3E+11
ω CUT 2.1E+01

B-10b

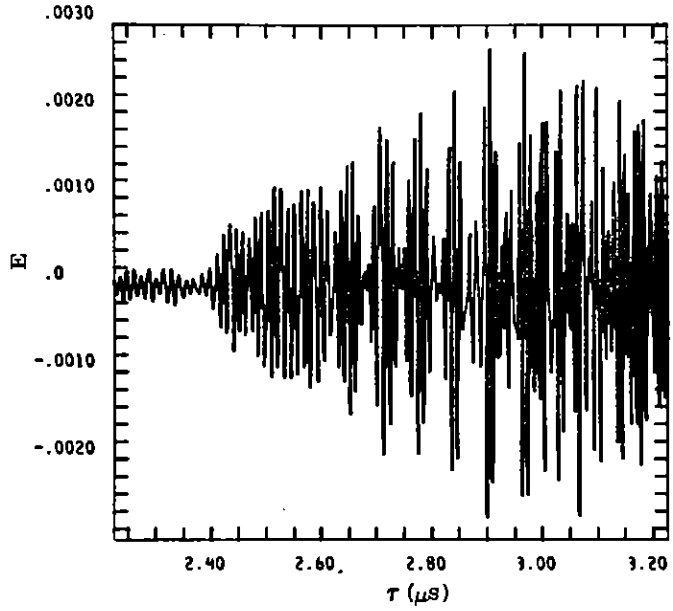

A= 4.0
B= 476.0
T= 1.0
K= 325.0
TEC = 7.0E+18
PEAK N 1.3E+11
ω CUT 2.1E+01

B-11a

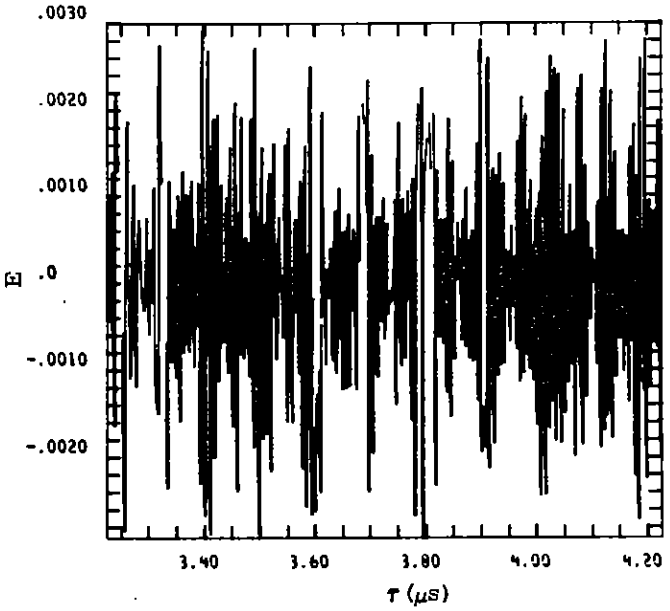

A= 4.0
B= 476.0
T= 1.0
K= 325.0
TEC = 7.0E+18
PEAK N 1.3E+11
ω CUT 2.1E+01

B-11b

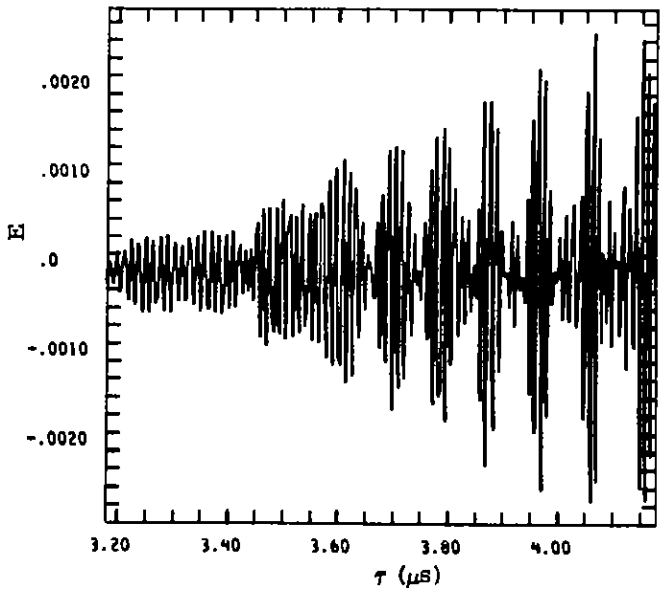

A= 4.0
B= 476.0
T= 1.0
K= 325.0
TEC = 1.0E+19
PEAK N 1.3E+11
ω CUT 2.1E+01

B-12a

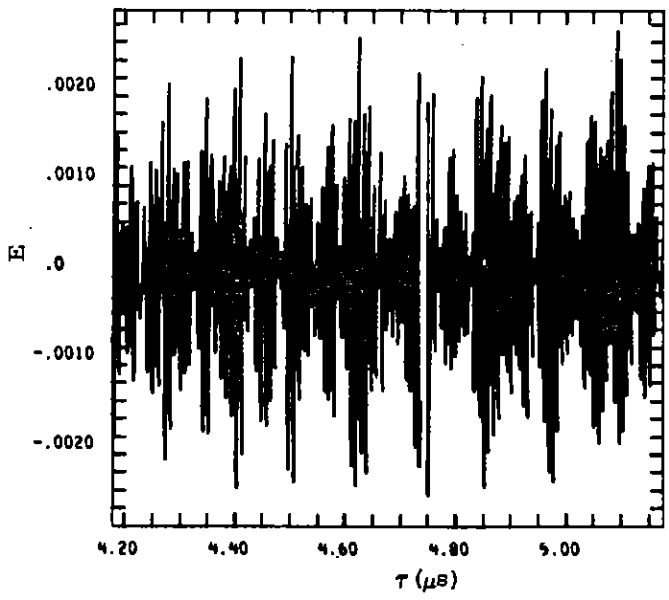

A= 4.0
B= 476.0
T= 1.0
K= 325.0
TEC = 1.0E+19
PEAK N 1.3E+11
ω CUT 2.1E+01

B-12b

Appendix C

EXAMINATION OF INDIVIDUAL FREQUENCY COMPONENTS

This appendix has been included in order to illustrate variation in the contributions of several quasi-monochromatic frequency components and the effect of the correction term in Eq. (30) that has been included to account for the possibility of low dispersion. The amplitude units are normalized to the 0.93 amplitude of the incident pulse. For these graphs K indicates the contribution of the k = K component. The resultant pulse is given in Appendix B for the TEC = 2.5×10^{15} electrons/m^2 case examined here. The correction terms have been multiplied by 10^6 as indicated. For the cases shown, the correction term is $\lesssim 6$ percent for each of the k values chosen. When results are displayed as in Figure 11 the correction term reduces f by a factor of ~ 2 for TEC = 2.5×10^{15} electrons/m^2.

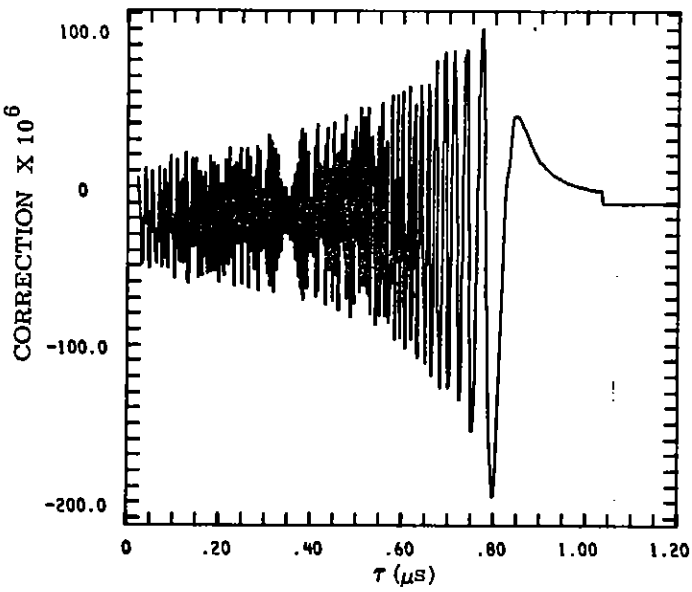

A= 4.0
B= 476.0
T= 1.0
K= 61.0
TEC = 2.5E+15
PEAK N 9.2E+10
ω CUT 1.7E+01

C-1a

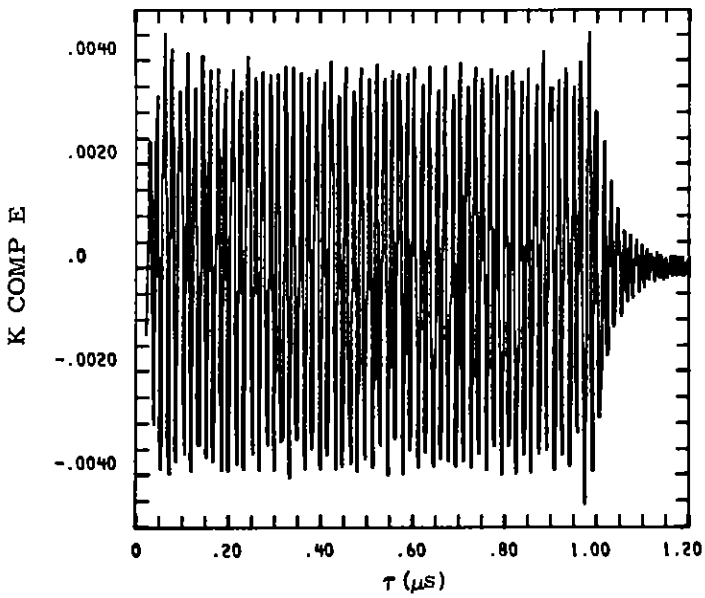

A= 4.0
B= 476.0
T= 1.0
K= 61.0
TEC = 2.5E+15
PEAK N 9.2E+10
ω CUT 1.7E+01

C-1b

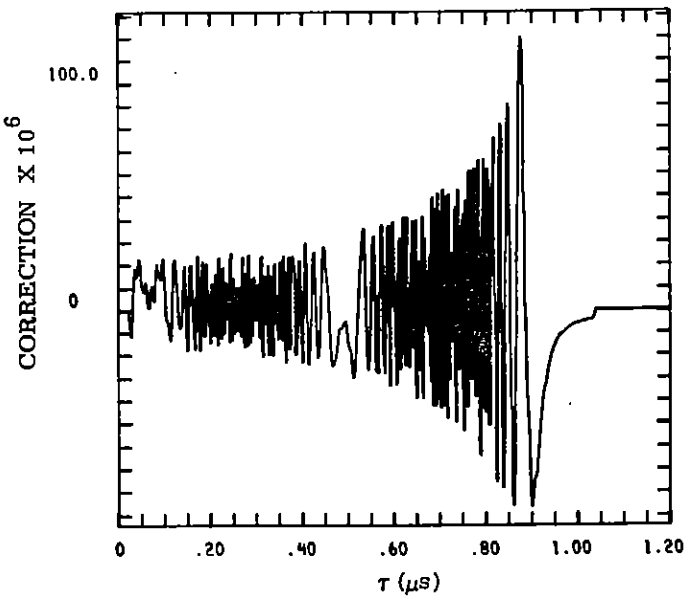

A= 4.0
B= 476.0
T= 1.0
K= 81.0
TEC = 2.5E+15
PEAK N 9.2E+10
ω CUT 1.7E+01

C-2a

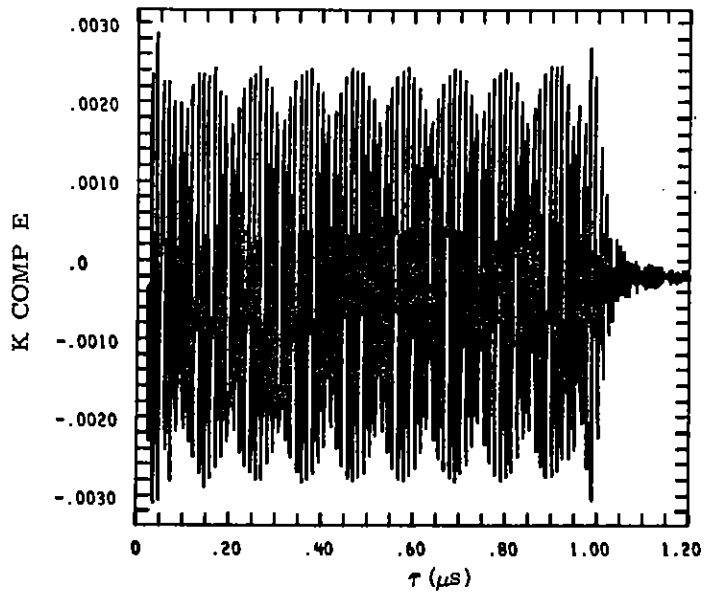

A= 4.0
B= 476.0
T= 1.0
K= 81.0
TEC = 2.5E+15
PEAK N 9.2E+10
ω CUT 1.7E+01

C-2b

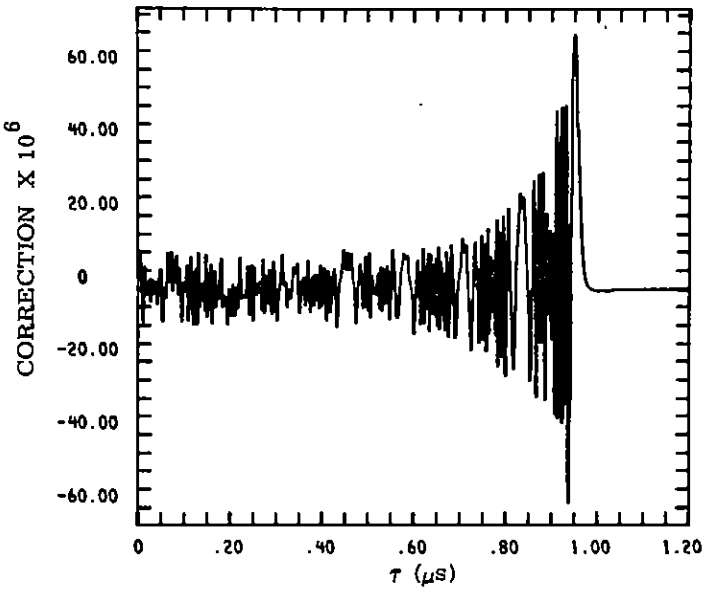

A= 4.0
B= 476.0
T= 1.0
K= 121.0
TEC = 2.5E+15
PEAK N 9.2E+10
ω CUT 1.7E+01

C-3a

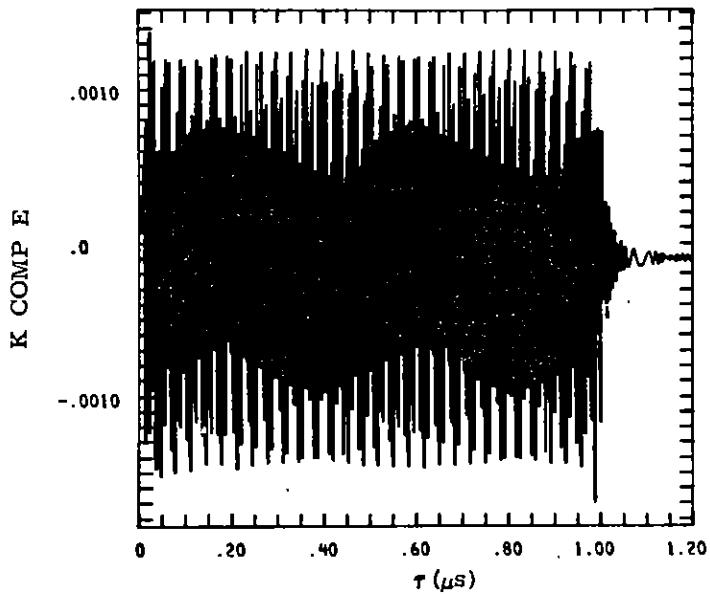

A= 4.0
B= 476.0
T= 1.0
K= 121.0
TEC = 2.5E+15
PEAK N 9.2E+10
ω CUT 1.7E+01

C-3b

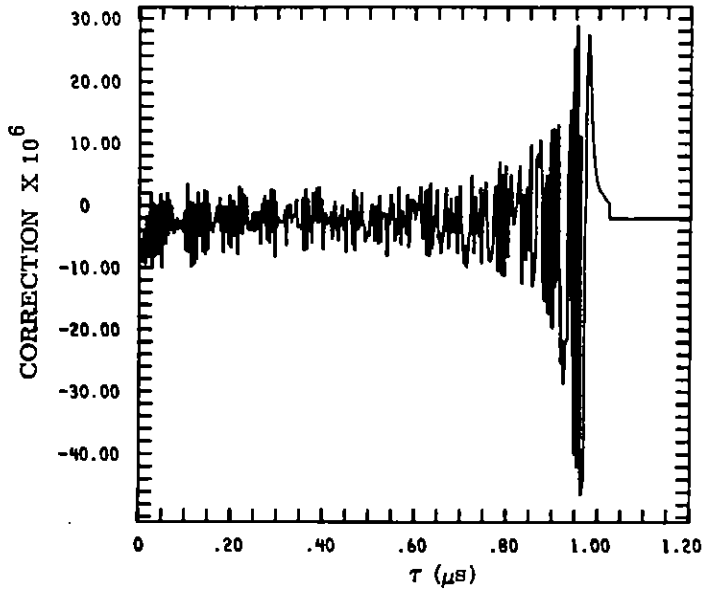

A= 4.0
B= 476.0
T= 1.0
K= 161.0
TEC = 2.5E+15
PEAK N 9.2E+10
ω CUT 1.7E+01

C-4a

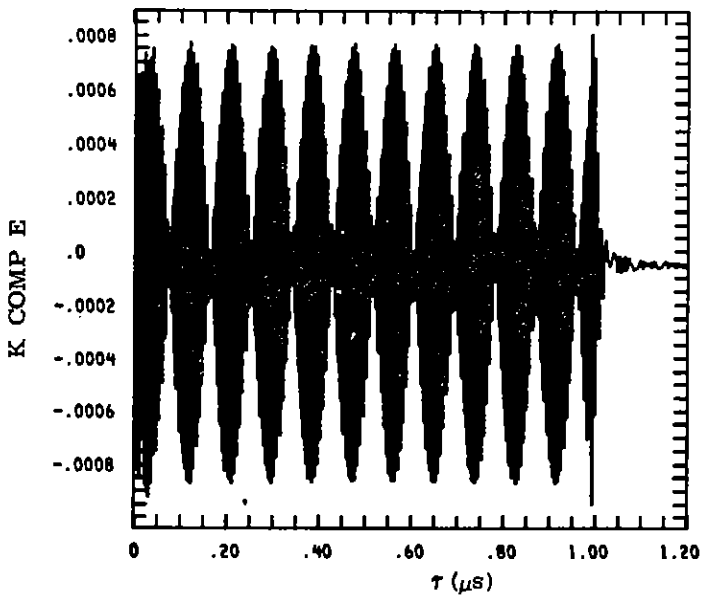

A= 4.0
B= 476.0
T= 1.0
K= 161.0
TEC = 2.5E+15
PEAK N 9.2E+10
ω CUT 1.7E+01

C-4b

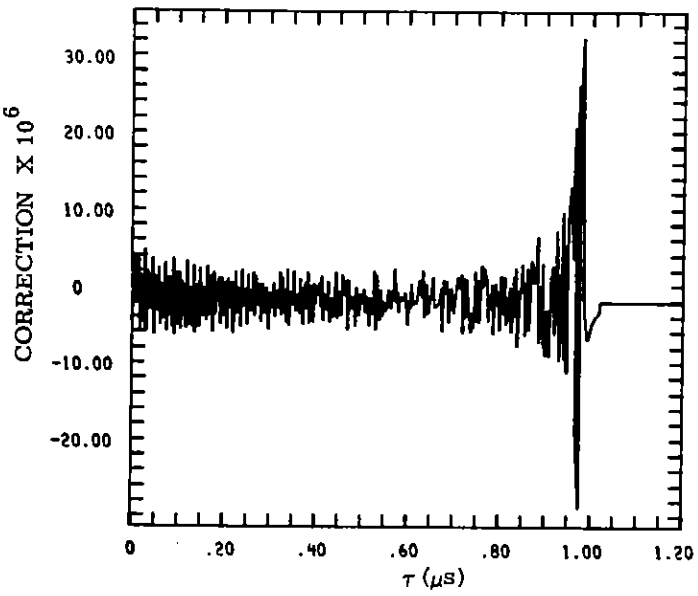

A= 4.0
B= 476.0
T= 1.0
K= 201.0
TEC = 2.5E+15
PEAK N 9.2E+10
ω CUT 1.7E+01

C-5a

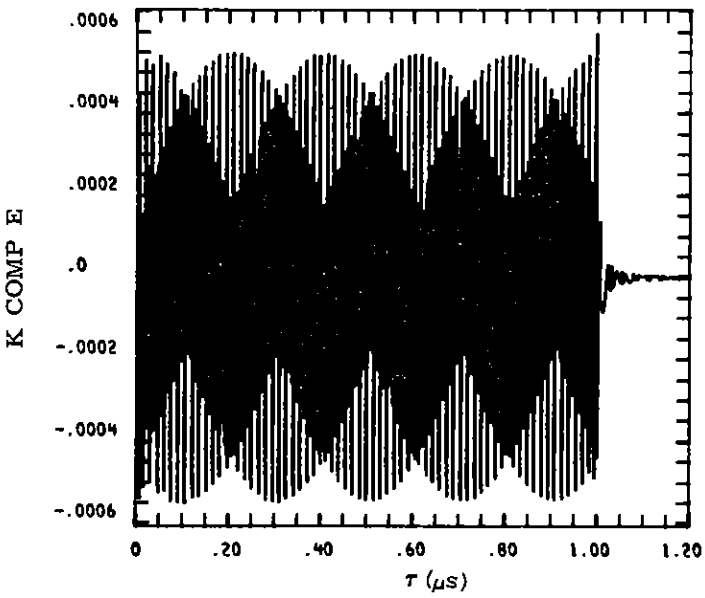

A= 4.0
B= 476.0
T= 1.0
K= 201.0
TEC = 2.5E+15
PEAK N 9.2E+10
ω CUT 1.7E+01

C-5b

REFERENCES

1. V. L. Ginzburg, The Propagation of Electromagnetic Waves in Plasmas, Pergamon Press, New York, 1970.

2. R. D. Jones and D. Z. Ring, Ionospheric Modification of the Electromagnetic Pulse From Nuclear Explosions, Sandia Laboratories report SC-RR-72 0400, July 1972.

3. M. A. Messier, "The Ionospherically Propagated Exoatmospheric EMP Environment," EMP Theoretical Note 163 of the AFWL, January 1973.

4. D. A. Dahlgren, L. T. Ritchie, and A. W. Shiver, The Sandia Satellite Vulnerability Model, unpublished report.

5. G. H. Price, Electromagnetic Pulse Propagation in the Ionosphere, AFWL-TR-69-71, January 1970.

6. F. Biggs and D. E. Amos, Numerical Solutions of Integral Equations and Curve Fitting, Sandia Laboratories report SC-RR-71 0212, September 1971.

7. R. S. Lawrence, C. G. Little, and H. J. A. Chivers, "A Survey of Ionospheric Effects Upon Earth-Space Radio Propagation," Proc. of IEEE 52, 4(1964).

8. C. B. Bailey and R. E. Jones, MATHLIB: A Brief User's Guide to the Sandia Mathematical Program Library, Sandia Laboratories report SC-M-72 0142, April 1972.

9. D. E. Merewether, J. A. Cooper, and R. L. Parker, eds, Electromagnetic Pulse Handbook for Missiles andAircraft in Flight, Sandia Laboratories report SC-M-71 0346, September 1972. This reference includes a detailed discussion of antenna response in Chapter 2.